ISSN 0016-7037
Volume 74, Number 17
September 1, 2010

ELSEVIER

Geochimica et Cosmochimica Acta

JOURNAL OF THE GEOCHEMICAL SOCIETY
AND THE METEORITICAL SOCIETY

Volume 74, Number 17 — September 1, 2010

Articles

Continued on outside back cover

Available online at www.sciencedirect.com
ScienceDirect
Geochimica et Cosmochimica Acta 74 (2010) 4953–4970
Geochimica et Cosmochimica Acta
www.elsevier.com/locate/gca

Sulfur cycling in a stratified euxinic lake with moderately high sulfate: Constraints from quadruple S isotopes

Aubrey L. Zerkle [a,*], Alexey Kamyshny Jr. [a,b,1], Lee R. Kump [c,2], James Farquhar [a,3], Harry Oduro [a,4], Michael A. Arthur [c,5]

[a] Department of Geology and Earth Systems Science Interdisciplinary Center, University of Maryland, College Park, MD 20742, USA
[b] Max Planck Institute for Marine Microbiology, Celsiusstrasse 1, Bremen 28359, Germany
[c] Department of Geosciences, Pennsylvania State University, University Park, PA 16802, USA

Received 25 September 2009; accepted in revised form 10 June 2010; available online 15 June 2010

Abstract

We present a 3-year study of concentrations and sulfur isotope values ($\delta^{34}S$, $\Delta^{33}S$, and $\Delta^{36}S$) of sulfur compounds in the water column of Fayetteville Green Lake (NY, USA), a stratified (meromictic) euxinic lake with moderately high sulfate concentrations (12–16 mM). We utilize our results along with numerical models (including transport within the lake) to identify and quantify the major biological and abiotic processes contributing to sulfur cycling in the system. The isotope values of sulfide and zero-valent sulfur across the redox-interface (chemocline) change seasonally in response to changes in sulfide oxidation processes. In the fall, sulfide oxidation occurs primarily via abiotic reaction with oxygen, as reflected by an increase in sulfide $\delta^{34}S$ at the redox interface. Interestingly, S isotope values for zero-valent sulfur sampled at this time still reflect production and recycling by phototrophic S-oxidation. In the spring, sulfide S isotope values suggest an increased input from phototrophic oxidation, consistent with a more pronounced phototroph population at the chemocline. This trend is associated with smaller fractionations between sulfide and zero-valent sulfur, suggesting a metabolic rate control on fractionation similar to that for sulfate reduction. Comparison of our data with previous studies indicates that the S isotope values of sulfate and sulfide in the deep waters are remarkably stable over long periods of time, with consistently large fractionations of up to 58‰ in $\delta^{34}S$. Models of the $\delta^{34}S$ and $\Delta^{33}S$ trends in the deep waters (considering mass transport via diffusion and advection along with biological processes) require that these fractionations are a consequence of sulfur compound disproportionation at and below the redox interface in addition to large fractionations during sulfate reduction. The large fractionations during sulfate reduction appear to be a consequence of the high sulfate concentrations and the distribution of organic matter in the water column. The occurrence of disproportionation in the lake is supported by profiles of intermediate sulfur compounds and by lake microbiology, but is not evident from the $\delta^{34}S$ trends alone. These results illustrate the utility of including minor S isotopes in sulfur isotope studies to unravel complex sulfur cycling in natural systems.

1. INTRODUCTION

The S isotope ratios of sulfur species in natural systems reflect the biological and geochemical processes that contribute to sulfur cycling in the environment. The biogeochemical sulfur cycle is primarily mediated by microbial processes, each of which is associated with a specific range of isotopic fractionations. Reduction of sulfate to sulfide by dissimilatory sulfate-reducing prokaryotes in anaerobic

* Corresponding author. Tel.: +1 301 405 2407.
E-mail addresses: azerkle@umd.edu (A.L. Zerkle), kamyshny@umd.edu (A. Kamyshny), lkump@psu.edu (L.R. Kump), jfarquha@Glue.umd.edu (J. Farquhar), hoduro@umd.edu (H. Oduro), arthur@geosc.psu.edu (M.A. Arthur).
[1] Tel.: +1 301 405 5009.
[2] Tel.: +1 814 863 1274.
[3] Tel.: +1 301 405 1116.
[4] Tel.: +1 301 405 6354.
[5] Tel.: +1 814 863 6054.

0016-7037/$ - see front matter © 2010 Elsevier Ltd. All rights reserved.
doi:10.1016/j.gca.2010.06.015

settings produces the majority of the isotopic signal. In laboratory experiments, pure cultures and mixed populations of sulfate reducers have generated sulfide that is up to 48‰ depleted in ^{34}S from reactant sulfate (Kaplan and Rittenberg, 1964; Canfield, 2001a; Habicht and Canfield, 2001). Isotope fractionation during sulfate reduction has been shown to vary not only with the organism (e.g., Detmers et al., 2001), but also with environmental parameters such as sulfate concentration, carbon or electron donor availability, and temperature (Harrison and Thode, 1958; Kaplan and Rittenberg, 1964; Habicht et al., 2002; Brüchert, 2004; Canfield et al., 2006). Fractionations between sulfate and sulfide in ancient sediments and in modern anoxic systems often exceed the maximum fractionations measured in experiments with sulfate reducers alone (up to 70‰; Fry et al., 1991; Canfield and Teske, 1996; Canfield, 2001b; Neretin et al., 2003). In some systems, these exceptionally large fractionations can be attributed to recycling of sulfide by oxidation and/or disproportionation reactions (Canfield and Thamdrup, 1994; Habicht et al., 1998; Sørensen and Canfield, 2004). Oxidation processes (e.g., phototrophic oxidation of sulfide with sunlight, or chemotrophic oxidation with oxygen or nitrate), produce small fractionations in $^{34}S/^{32}S$ (0–5‰; Fry et al., 1984, 1986, 1988). Biological disproportionation of intermediate sulfur compounds (zero-valent sulfur, SO_3^-, and $S_2O_3^{2-}$) to sulfide and sulfate can generate additional larger fractionations, with product H_2S generally depleted in ^{34}S by 5–7‰, and product SO_4^{2-} generally enriched in ^{34}S by 17–21‰ (Canfield, 2001a). Numerical models of sediment sulfur isotopes (Goldhaber and Kaplan, 1980; Wortmann et al., 2001) and of the sulfate reduction metabolism (Brunner and Bernasconi, 2005) have additionally suggested that sulfate reducers are capable of producing much larger fractionations than what has been measured experimentally, perhaps explaining the large fractionations observed in nature without invoking additional oxidative cycling. These large fractionations have only recently been demonstrated in incubations with natural populations of sulfate reducers (Canfield et al., 2010).

Meromictic (permanently stratified) lakes provide unique environments in which to study sulfur transformations, particularly those involved in the oxidative part of the sulfur cycle. In these environments, density stratification of the water column typically results in an upper, well-oxygenated mixed water mass (*mixolimnion*), overlying a stagnant anoxic deep water mass (*monimolimnion*). Given sufficient sulfate, sulfate reduction can occur throughout the anoxic deep waters, leading to the buildup of hydrogen sulfide and euxinic conditions. The redox interface between oxic and sulfidic waters (the *chemocline*) in these systems harbors steep geochemical gradients and is an intense zone of sulfide oxidation (e.g., Mandernack and Tebo, 1999). If the chemocline occurs in the photic zone, these environments often support a dense community of phototrophic sulfur oxidizing bacteria that can sustain high levels of nutrient cycling and primary productivity rivaling that of the epilimnion of dimictic lakes (e.g., Overmann et al., 1991; Overmann, 1997; Canfield et al., 2005).

Previous workers have measured $\delta^{34}S$ of sulfur compounds in stratified systems as a proxy for sulfur cycling processes. Studies of the $\delta^{34}S$ of sulfide in euxinic Mariager Fjord demonstrated that most of the sulfide accumulating in the fjord was formed in the sediments (presumably via sulfate reduction), but the isotopic composition of sulfide within the water column was affected by further oxidative processes, such as disproportionation (Sørensen and Canfield, 2004). These researchers also demonstrated that the $\delta^{34}S$ composition of sulfide in Mariager Fjord fluctuated in response to periods of net sulfide oxidation and sulfate reduction in the basin. The $\delta^{34}S$ of sulfur compounds in the Black Sea water column has been investigated by a number of workers (Sweeney and Kaplan, 1980; Lein and Ivanov, 1990; Fry et al., 1991; Muramoto et al., 1991; Neretin et al., 1996, 2003). These studies documented an enrichment in ^{34}S in sulfide near the chemocline, due to either sulfide oxidation or decreased fractionation during high rates of sulfate reduction at the chemocline. Mandernack et al. (2003) similarly suggested that decreasing sulfate $\delta^{34}S$ at the redox interface of Framvaren Fjord was due to sulfide oxidation, with a zone of sulfur disproportionation just below indicated by higher sulfate $\delta^{34}S$ and $\delta^{18}O$.

A number of studies have examined the $\delta^{34}S$ of sulfur compounds (primarily pyrite) in the sediments of euxinic environments, to distinguish diagenetic pyrite formed in the sediments from syngenetic pyrite formed in the water column (Lyons, 1997; Wilkin and Barnes, 1997; Suits and Wilkin, 1998; Lyons et al., 2003; Werne et al., 2003; Donahue et al., 2008). These studies were primarily undertaken in an attempt to evaluate the validity of using $\delta^{34}S$ of ancient sedimentary pyrite to infer conditions in the water column during formation, and the results were highly variable. For example, a low percentage of syngenetic pyrite was found in sediments from Fayetteville Green Lake, NY (Suits and Wilkin, 1998), in contrast to the Black Sea, where nearly all of the sedimentary pyrite appeared to be syngenetic (Lyons, 1997). The differences in pyrite formation were concluded to arise from variations in the physical and chemical properties of sedimentation in the basin, along with the physical, chemical, and biological conditions in the chemocline (Suits and Wilkin, 1998; Werne et al., 2003).

The above studies have demonstrated the utility of $\delta^{34}S$ in understanding sulfur cycling in stratified systems. However, uncertainties still remain as to the relative roles of sulfate reduction, sulfur compound disproportionation, and sulfide oxidation in sulfur cycling, and in controlling the isotopic composition of sulfur in the environment. Minor sulfur isotopes (^{33}S and ^{36}S) are providing a new and powerful tool in reconstructing biogeochemical cycles in modern and ancient systems. These minor isotopes are subject to inorganic and organic fractionation mechanisms that are similar to those for ^{34}S. In addition, the redistribution of multiple S isotopes within biogeochemical systems (at both the cellular and ecosystem level) produces unique patterns that can be used to assess the contribution of different pathways (enzymatic or biogeochemical) to the measured isotopic values. Previous experimental studies have shown that biological S metabolisms produce characteristic minor isotope patterns, which arise from differences in the individual steps controlling the material flow through the metabolic pathways (Farquhar et al., 2003, 2007; Johnston et al., 2005a, 2007, 2008a; Ono

et al., 2006; Zerkle et al., 2009). These isotope patterns have been utilized in models examining the sulfur cycle in natural systems (Farquhar et al., 2008; Johnston et al., 2008a; Zerkle et al., 2009), and used to interpret sulfur isotope signatures in ancient sediments (Johnston et al., 2005b, 2006, 2008b).

One recent focus in multiple sulfur isotope studies is on gauging their utility in describing sulfur cycling in modern environments (Farquhar et al., 2007, 2009; Gilhooly et al., 2009; Canfield et al., 2010). In this regard, we present measurements of the concentrations and isotopic values of sulfate, sulfide, and intermediate S species in meromictic Fayetteville Green Lake (FGL), and utilize the patterns we see to constrain the involvement of different sulfur metabolisms in the lake's sulfur cycle. Additionally, we use a depth-derived model of sulfide in the deep waters to assess the contribution of physical processes (diffusion and advection) and biogeochemical processes (sulfate reduction, sulfur compound disproportionation, and sulfide oxidation) to the isotopic composition of sulfide in the lake. FGL is a model system for this type of study because it is one of the most well-studied meromictic lakes in the US (with literature dating back to the mid-1800s; Vanuxem, 1839), it has a thriving microbial ecosystem (including a large population of phototrophic S-oxidizing organisms at the chemocline; Thompson et al., 1990), and large fractionations in $\delta^{34}S$ have previously been measured between sulfide and sulfate in the water column (Deevey et al., 1963; Fry, 1986).

2. STUDY AREA

Fayetteville Green Lake (FGL) is a small (0.26 km^2), permanently stratified lake located in Green Lakes State Park, approximately 20 km east of Syracuse, near the town of Fayetteville, New York, USA (Brunskill and Ludlam, 1969) (Fig. 1). FGL has a long history of scientific study dating back to the mid-1800s (Vanuxem, 1839; Brunskill, 1969; Brunskill and Harriss, 1969; Brunskill and Ludlam, 1969; Culver and Brunskill, 1969; Ludlam, 1969). More recently, the lake has been the subject of intense study due to its extensive accumulations of benthic calcium carbonate bioherms and perennial "whiting" events of carbonate precipitation in surface waters (Thompson and Ferris, 1990; Thompson et al., 1990, 1997).

FGL occupies a deep (~52 m) basin in the lower unit of the Silurian Syracuse Formation and Vernon Shale. This steep-sided plunge basin was carved out by glacial waterfalls during the late Wisconsinan glaciations (Muller, 1967). Over 50% of the lake's water supply comes from ground water sources, and the rest is from surface runoff (Brunskill and Ludlam, 1969). Calcium- and sulfate-rich groundwater enters the lake at ~16–18 m depth, corresponding to the contact between the green and red shale facies of the gypsum-rich Vernon shale (Brunskill and Ludlam, 1969). This saline groundwater input maintains density stratification and elevated sulfate levels (12–15 mM) (Takahashi et al., 1968; Brunskill and Ludlam, 1969; Torgersen et al., 1981; Thompson et al., 1990). The large sulfate input additionally supports high rates of microbial sulfate reduction, leading to the buildup of over 1 mM H_2S in the deep waters, and the development of a sharp oxic–anoxic interface at around 18–21 m depth (Brunskill, 1969; Brunskill and Ludlam, 1969). The chemocline at FGL harbors a dense and productive community of phototrophic S-oxidizing bacteria, consisting of both green

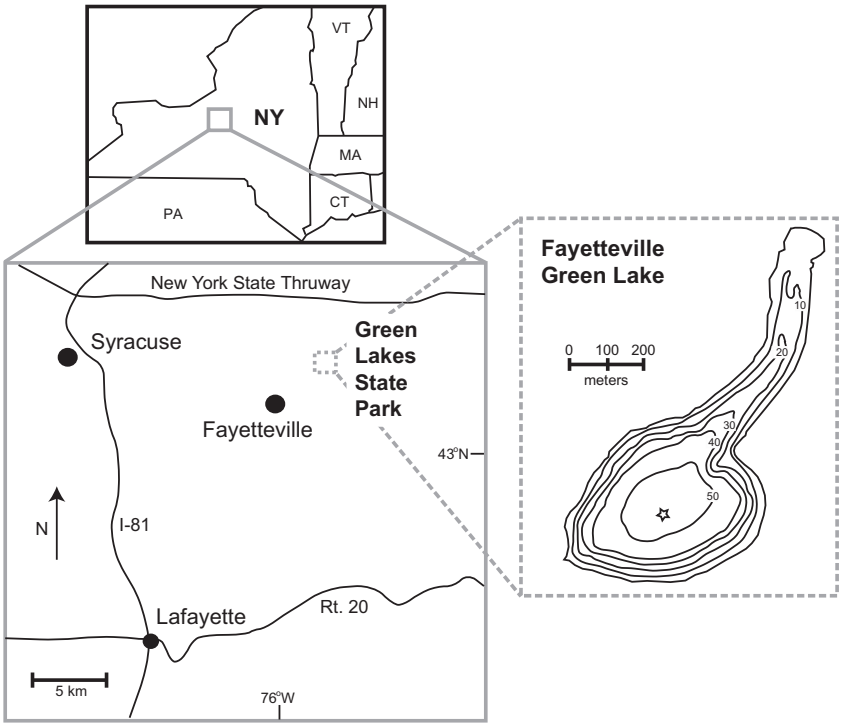

Fig. 1. Location of Fayetteville Green Lake in upstate NY, USA, and lake bathymetry (from Brunskill and Ludlam, 1969). Star symbol indicates approximate sampling position.

and purple sulfur bacteria (Culver and Brunskill, 1969; Thompson et al., 1990). The remainder of primary productivity in the lake is due to oxygenic phototrophs (*Synechococcus* sp.) that populate the upper oxygenated water column and are suggested to be responsible for the bioherms and whiting events (Thompson and Ferris, 1990; Thompson et al., 1990).

Previous studies have measured the isotopic composition of sulfur species in FGL (Deevey et al., 1963; Fry, 1986), and reported large fractionations between sulfate and sulfide in the water column (56–57.5‰). Here, we expand upon these previous $\delta^{34}S$ measurements, and include measurements of $\Delta^{33}S$ and $\Delta^{36}S$, as well as a seasonal comparison between isotopic values in the fall (October–November) and in the spring (April–May).

3. METHODS

Most of the field work for this study was completed in October, 2008 (at the end of a seasonal whiting event), and in April–May, 2009 (just before). Samples of sulfide and sulfate for isotope analysis were also collected during a field excursion in November, 2006 (Riccardi, 2007). Geochemical profiles (depth, temperature, pH, specific conductivity, turbidity, and oxygen concentration) were taken *in situ* with a YSI 6600 multiparameter sonde.

Samples for sulfate concentrations (taken in November) were filtered through a 0.45 μm in-line filter, immediately precipitated with $BaCl_2$ as $BaSO_4$, filtered and dried. Sulfate concentrations were determined gravimetrically (analytical error of ~2%). Samples for sulfide concentrations and isotopes were taken directly in 1:10 (by volume) 1 M Zn-acetate and analyzed by the colorimetric methylene-blue method (Cline, 1969). We estimate a total of ~11.5% error on sulfide measurements (10% sampling error + 1.5% analytical error). Sulfide and sulfate isotope samples were filtered to capture ZnS, then 1 M $BaCl_2$ was added to precipitate $BaSO_4$, then samples were filtered again to capture $BaSO_4$. ZnS and $BaSO_4$ captured on filters was frozen at −20 °C and stored for less than 2 weeks. Filtering of ZnS also captured biomass and other particulates (particularly across the chemocline), and therefore samples for sulfide isotopes were redistilled to H_2S by the acid-volatile sulfur method (boiling in 5 M HCl), which volatilizes zinc-sulfide but not zero-valent sulfur or organically bound sulfur. $BaSO_4$ was reduced to H_2S gas by boiling in a solution of 320 ml HI, 524 ml HCl, and 156 ml H_2PO_4 per l (Forrest and Newman, 1977). In both reactions, H_2S gas was trapped as ZnS with Zn-acetate and converted to Ag_2S with drop-wise addition of $AgNO_3$. Ag_2S was cleaned with 350 ml of Milli Q water and 50 ml of 1 M NH_4OH and dried overnight.

Samples for zero-valent sulfur quantification (elemental sulfur + polysulfides, herein referred to as "ZVS") were taken in triplicate (40 ml sample added to 4 ml of 5% Zn-acetate) and frozen immediately in dry ice. In October, select samples were additionally filtered through 0.45 μm and 0.2 μm syringe filters to distinguish between particle-associated ZVS and dissolved ZVS. Immediately before analysis samples were thawed, an internal standard (40 μl of 400 mg/l solution of 4,4′-dibrombiphenyl in methanol) was added, and samples were extracted twice with 2 ml of chloroform. ZVS concentrations were measured on an Agilent Technologies 1100 HPLC system with multiple wavelength UV–vis detector, following methods adopted from Kamyshny et al. (2009). Samples for ZVS isotope measurements (900 ml) were added to 100 ml of 5% zinc acetate solution and immediately frozen in dry ice. In the laboratory, samples were thawed and extracted three times by 100 ml of chloroform, dried with calcium chloride, filtered, and evaporated to 0.5–1 ml volume. Concentrated samples for isotope analyses were either reduced to H_2S utilizing a Cr(II) reduction solution in water with ethanol (according to Gröger et al., 2009), or purified by preparative HPLC (as in Kamyshny et al., 2009) and reduced to H_2S by reaction with a highly active Raney–Nickel catalyst. Raney–Nickel reactions were performed using a method modified from Granatelli (1959). Briefly, 0.8 g of freshly prepared Raney–Nickel catalyst was introduced into a clean three-neck round-bottom flask containing 15 ml of methanol solution and ZVS sample. The solution was first purged with N_2, then 0.5 ml of a 1.5 mol/l NaOH solution was added by to the flask by syringe. The flask content was boiled for 15 min under N_2, cooled to room temperature, and then concentrated HCl was added drop-wise into the reaction flask. The reaction mixture was heated a final time to release the converted H_2S gas, which was immediately precipitated with $AgNO_3$ to Ag_2S for isotopic analysis. Mean recovery for repeat reductions of ZVS using this method was 94 ± 2%.

Samples for thiosulfate and sulfite analysis (0.5 ml) were added to 50 μl of 5% zinc acetate and frozen immediately in dry ice. All samples were taken in triplicates. In the laboratory, samples were thawed and immediately derivatized by monobromobimane and analyzed by HPLC with fluorescence detector following the method of Zopfi et al. (2004), with the exception that a 250 mm column was used for separation.

For fluorination, Ag_2S was reacted in Ni bombs with 10× excess F_2 gas at ~250 °C for ~8 h, to quantitatively convert the Ag_2S to SF_6. Product SF_6 was purified cryogenically by distillation in a liquid N_2-ethanol slurry at −115 °C, and by gas chromatography on a 12′ molecular sieve 5 Å/Hasep Q column with a TCD. The isotopic abundance of the purified SF_6 was analyzed on a Finnigan MAT 253 dual inlet mass spectrometer at *m*/*e*- values of 127, 128, 129, and 131 ($^{32}SF_5^+$, $^{33}SF_5^+$, $^{34}SF_5^+$, and $^{36}SF_5^+$). We use values for IAEA-S1 on the VCDT normalization of −0.30‰, 0.94‰, and −0.7‰ for $\delta^{34}S$, $\Delta^{33}S$, and $\Delta^{36}S$. Analytical uncertainties on S isotope measurements, estimated from long-term reproducibility of Ag_2S fluorinations, are 0.14, 0.008, and 0.20 (1σ) for $\delta^{34}S$, $\Delta^{33}S$, and $\Delta^{36}S$, respectively.

The ^{3X}S isotopic composition of sulfur species (in permil, ‰) is presented using the standard delta (δ) notation:

$$\delta^{3X}S = \left[\left({}^{3X}R_{sample}/{}^{3X}R_{VCDT}\right) - 1\right] \quad (1)$$

where $^{3X}R_{sample}/^{3X}R_{VCDT}$ is the isotopic ratio of a sample ($^{3X}R = {}^{3X}S/{}^{32}S$ for 3X = 33, 34, or 36) relative to the Vienna-Cañon Diabolo Troilite (VCDT) standard. We define

the fractionation factor between two sulfur species, α, using the following equation:

$$^{3X}\alpha_{A-B} = \frac{^{3X}R_A/^{3X}R_{VCDT}}{^{3X}R_B/^{3X}R_{VCDT}}. \quad (2)$$

The minor isotope compositions of sulfur species are presented using the $\Delta^{3X}S$ notation, which describes the deviation of a sample datum in ^{33}S or ^{36}S (in ‰) from a reference fractionation line:

$$\Delta^{33}S = \delta^{33}S - \left[\left(^{34}R_{sample}/^{34}R_{VCDT}\right)^{0.515} - 1\right] \quad (3)$$

and

$$\Delta^{36}S = \delta^{36}S - \left[\left(^{34}R_{sample}/^{34}R_{VCDT}\right)^{1.90} - 1\right] \quad (4)$$

The exponents 0.515 and 1.90 are reference values assigned to approximate mass-dependent fractionations during thermodynamic equilibrium isotope exchange at low temperature (Hulston and Thode, 1965; Farquhar et al., 2003; Farquhar and Wing, 2003; Johnston et al., 2007; Ono et al., 2007). Small deviations from these reference values occur in biogeochemical systems because the redistribution of mass between sulfur pools by, e.g., mixing or Rayleigh processes, results in the isotope ratios of sulfur pools evolving in a linear fashion according to:

$$(^{3X}S/^{32}S)_{tot} = {}^{32}X_a(^{3X}S/^{32}S)_a + {}^{32}X_b(^{3X}S/^{32}S)_b \quad (5)$$

where a and b are distinct pools of sulfur (e.g., sulfate and sulfide) with isotope ratios $^{3X}S/^{32}S$ (for ^{33}S, ^{34}S, and ^{36}S), and ^{32}X is the fraction of ^{32}S sulfur existing in each of the pools. This linear relationship differs from that calculated for reference fractionation arrays, which follows an exponential trend, as in:

$$(^{33}S/^{32}S)_a/(^{33}S/^{32}S)_b \sim [(^{34}S/^{32}S)_a/(^{34}S/^{32}S)_b]^{0.515} \quad (6)$$

for ^{33}S. For a more detailed explanation of how these signatures are produced in natural systems, see explanations in Farquhar et al. (2003, 2007) and Johnston et al. (2005a, 2007). The exponent characterizing these deviations is defined theoretically as θ:

$$^{3X}\theta = \frac{\ln {}^{3X}\alpha}{\ln {}^{34}\alpha} \quad (7)$$

for $^{33}\theta$ and $^{36}\theta$. This exponent can also be calculated from measured data (experimental or environmental samples, e.g., between sulfide and sulfate pairs) using the equation:

$$^{3X}\lambda_{A-B} = \frac{\ln(^{3X}R_A/^{3X}R_{VCDT}) - \ln(^{3X}R_B/^{3X}R_{VCDT})}{\ln(^{34}R_A/^{34}R_{VCDT}) - \ln(^{34}R_B/^{34}R_{VCDT})} \quad (8)$$

4. RESULTS

Profiles of temperature, pH, specific conductivity, and turbidity for the lake during October and April are shown in Fig. 2. Temperature reaches a maximum of ~16.5 °C in October at a depth of about 10 m, but in April only reaches ~15 °C in the top ~2 m. In April, we observed the pronounced temperature increase around the chemocline that has been previously described (Brunskill and Ludlam, 1969). Temperature in the monimolimnion was constant, at around 8 °C. pH was 7.6–8 in the surface waters, decreasing to a constant 6.5 in the deep waters. Specific conductivity was around 3.7–4 mS cm^{-1} in the surface waters, increasing to ~5 mS cm^{-1} at around 16 m, coinciding with the depth of the primary groundwater input (Brunskill and Ludlam, 1969). Turbidity remained near zero in the surface and deep waters, with a sharp increase in the chemocline around the area of visible pink water. This turbidity maximum was enhanced during the sampling before the whiting event, from to ~60 NTU in October to ~90 NTU in April.

Fig. 3 shows profiles of dissolved oxygen and sulfur species. O_2 begins to sharply decline at around 15 m, to 2–8% O_2 saturation from 20 to 22 m, then to 0% below 22 m. Sulfate increases from 12 to 16 mM from the mixolimnion to the monimolimnion (in the range of previous sulfate concentration measurements; Deevey et al., 1963; Brunskill and Ludlam, 1969), exhibiting a subtle maximum around 19–20 m. Sulfide concentrations were within estimated error between the two sampling periods, appearing at around 20 m and increasing with depth to 1.5–1.8 mM near the sediment–water interface. ZVS peaked around the chemocline, to >30 μM in October and >40 μM in April. Filtration of ZVS samples through 0.45 μm and 0.2 μm pore-size filters in October indicated that ZVS pools within the water column show very different particle size distributions (Fig. 4). At 20.5 m depth in the chemocline, where total ZVS concentration is the highest (31.1 μM), none of the ZVS passed a 0.45 μm filter. At 22 m depth just below the chemocline, nearly all of the ZVS passed through a 0.45 μm filter but not a 0.2 μm filter (>90%). In the deep waters near the sediment–water interface (44.1 m), most of the ZVS passed through a 0.2 μm filter (87%). At 46.6 m depth, the deepest point sampled, around 70% passed through a 0.45 μm filter and ~50% passed through a 0.2 μm filter. Thiosulfate and sulfite concentrations in FGL were very low (less than 1 μM), with the exception of one anomalously high thiosulfate value of ~3.4 μM at 45 m depth in April.

The $\delta^{34}S$, $\Delta^{33}S$, and $\Delta^{36}S$ values of sulfate, sulfide, and ZVS from the FGL water column are listed in Table 1 and shown in Fig. 5. The isotope values of sulfate and sulfide are remarkably similar for all three sampling intervals examined here, and also consistent with $\delta^{34}S$ values reported in previous studies (Deevey et al., 1963, sampled in June, and Fry, 1986, sampling season not reported). The one exception is that we see an increase of 1–4‰ in sulfide $\delta^{34}S$ at the oxic/anoxic interface, rather than the small decrease of ~1‰ previously measured (Fry, 1986). We also see very large fractionations in $\delta^{34}S$ between sulfate and sulfide in the FGL monimolimnion (calculated here as $(^{34}\alpha - 1) * 1000$), during both the fall season (49–56‰) and in the spring (53–58‰), similar to fractionations reported in Deevey et al. (1963) and Fry (1986) (mean of 56–56.5‰). Lambda values calculated between sulfate and sulfide in the FGL water column (using Eq. (8)) range from 0.5119 to 0.5134 for $^{33}\lambda$, and from 1.9225 to 1.9341 for $^{36}\lambda$, with a $\Delta^{36}S/\Delta^{33}S$ slope −10.6, which is within the range of mass-dependent relationships predicted for natural systems (Johnston et al., 2007).

ZVS samples collected from the chemocline in October have $\delta^{34}S$ values of −19.6‰, which is 6–7‰ more enriched

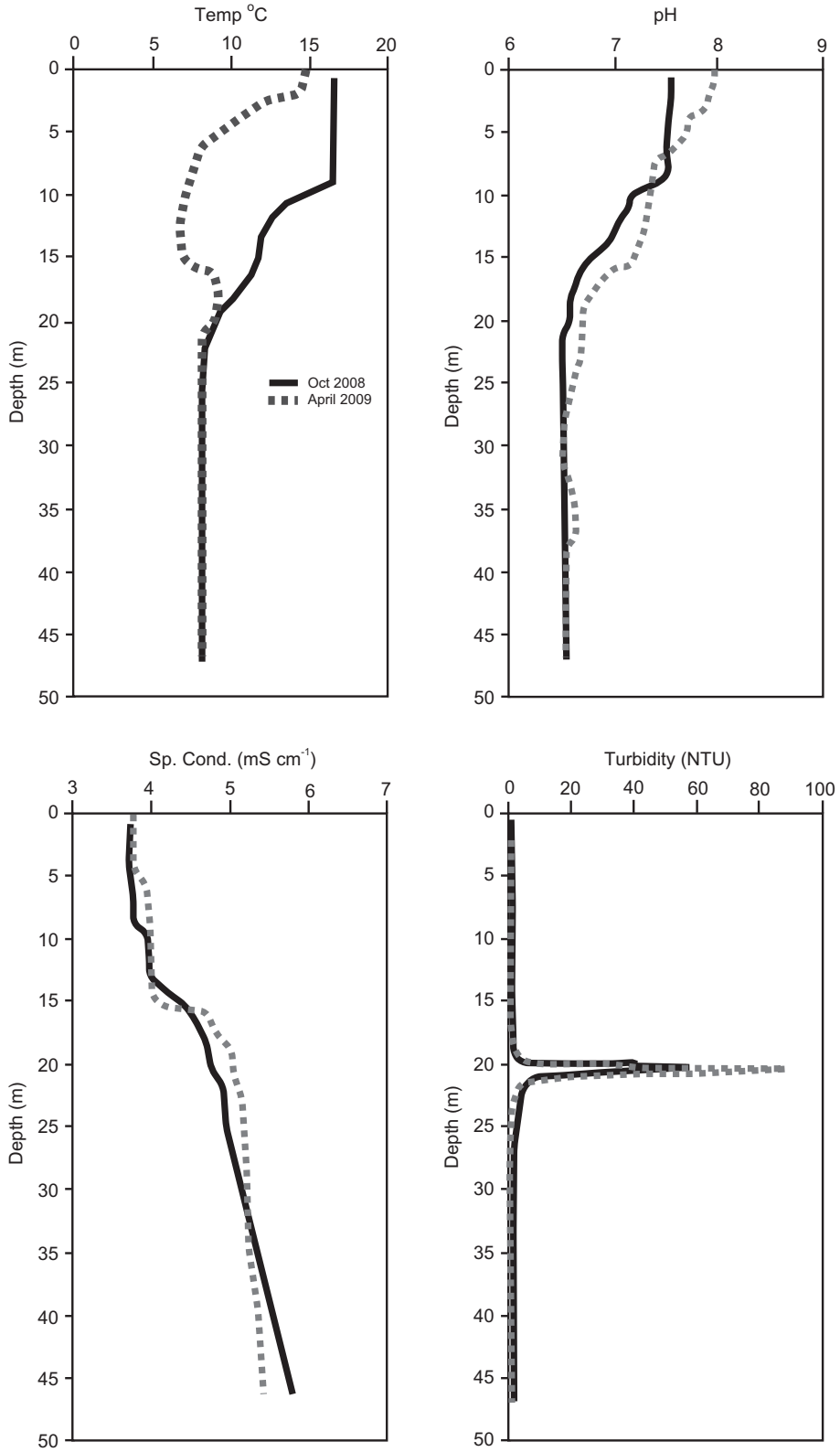

Fig. 2. *In situ* geochemical profiles for October, 2008, and April, 2009.

in ^{34}S than sulfide from the same sampling horizon (Fig. 5). The $\Delta^{33}S$ value of ZVS sampled at the top of the chemocline in October is similar to that of the surrounding sulfide (0.120‰), while ZVS sampled at the horizon with the high-

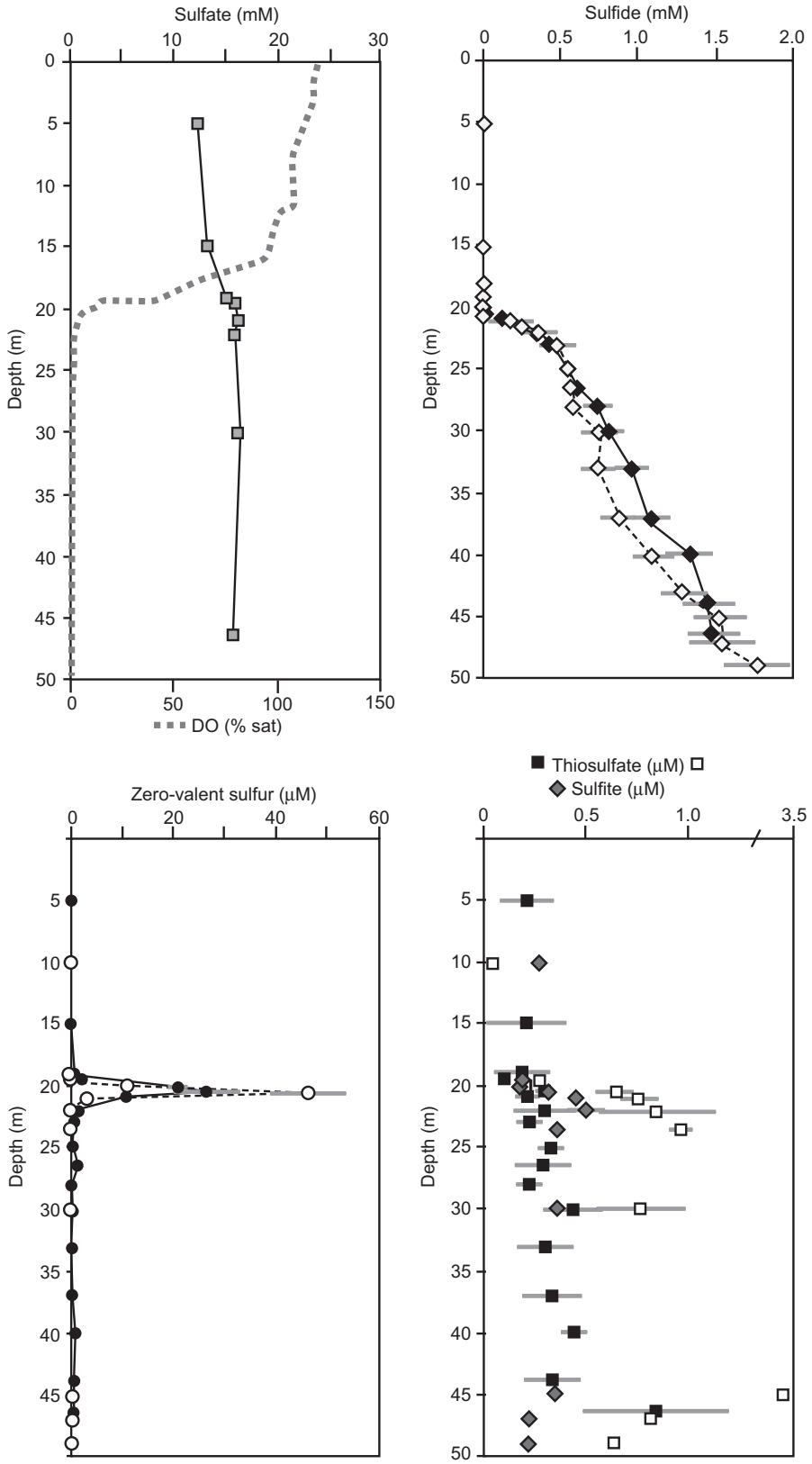

Fig. 3. Measurements of sulfur species in the lake. Sulfate data is from November, 2006, sulfite data is from April, 2009. For other sulfur species solid symbols are from October, 2008, and empty symbols are from April, 2009. Error bars represent standard deviations of sulfide, zero-valent sulfur, sulfite, and thiosulfate measurements made in triplicate, or estimated uncertainty of sulfide measurements (11.5%) if larger than standard deviations.

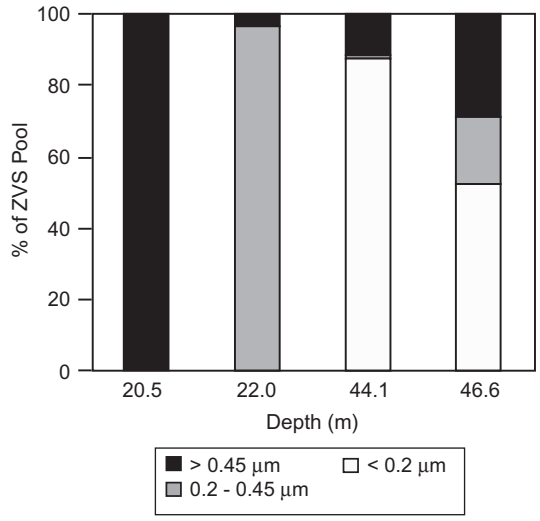

Fig. 4. Particle size distribution of ZVS samples from October, 2008, based on filtration through 0.45 and 0.2 µm pore-size filters. At the chemocline ZVS exists as large particulates, likely biologically associated (i.e., intracellular). At 22 m the ZVS is mostly smaller extracellular particulates. Deeper in the water column the ZVS is predominantly in the form of dissolved polysulfides, although large particles near the sediment–water interface (at 47 m) could indicate some sediment resuspension.

est turbidity (20.5 m) has a much smaller $\Delta^{33}S$ (0.017‰). Sulfide sampled at this depth has significantly smaller $\Delta^{33}S$ (0.088‰) and significantly larger $\Delta^{36}S$ (−1.207‰) as well. In April, ZVS had $\delta^{34}S$ values only about 1‰ more enriched in ^{34}S than sulfide, and a smaller correlative decrease in $\Delta^{33}S$ (to 0.106‰). $\Delta^{36}S$ values of ZVS from April look similar to that of sulfide (−1.3‰ to −1.5‰).

5. DISCUSSION

5.1. Sulfide oxidation at the chemocline

We examined the concentrations and isotopic values of sulfur species at the chemocline to determine which pathways are important in sulfide oxidation and how these processes are affected by changes in the phototroph community caused by the summer whiting event. Experimental evidence indicates that different sulfide oxidation processes produce distinct sulfur products and small but distinct isotope effects in $\delta^{34}S$. Most notably, biological oxidation of sulfide by anoxygenic phototrophic S-oxidizing organisms produces ZVS that is enriched in ^{34}S by 2–4‰, leading to an overall decrease in sulfide $\delta^{34}S$ values (Fry et al., 1986). Abiotic reaction of sulfide with oxygen, on the other hand, produces a mixture of ^{34}S-depleted products, resulting in an increase in sulfide $\delta^{34}S$ of up to 5‰ (Fry et al., 1988). Other oxidation reactions have been shown to produce negligible fractionations (<1‰, e.g., oxidation of sulfide by chemotrophic S-oxidizers or with Fe-oxides; Goldhaber and Kaplan, 1975; Fry et al., 1986).

In October, after a whiting event, sulfide $\delta^{34}S$ values at the chemocline of FGL were approximately 4‰ more enriched in ^{34}S than values from sulfide sampled directly below this horizon (Table 1 and Fig. 5). This increase in sulfide $\delta^{34}S$ at the chemocline suggests that sulfide oxidation (and the isotopic composition of sulfide at the chemocline) at this sampling were primarily controlled by abiotic reaction of sulfide with oxygen. Oxidation of sulfide with O_2 at near neutral pH produces a mixture of products, dominated by sulfate with minor production of sulfite and thiosulfate (Zhang and Millero, 1993). Sulfate is depleted in ^{34}S by approximately 3‰ at the redox interface (from 20 to 22 m) compared to $\delta^{34}S$ values measured lower in the monimolimnion (at >25 m) (Table 1), supporting the production of ^{34}S-depleted sulfate by this reaction. In April before a whiting event, the enrichment in ^{34}S of sulfide at the chemocline was less pronounced than in October (only ~2‰), which could reflect a greater contribution from phototrophic oxidation processes at this sampling. Phototrophic oxidation would presumably be enhanced due to greater light availability before a whiting event, as evidenced by a more dense community of phototrophs at the chemocline during this time.

Sulfur isotope values of ZVS at the chemocline provide insight into oxidation processes as well (Table 1 and Fig. 5). In October, ZVS was enriched in ^{34}S by 6–7‰ relative to sulfide from the same sampling horizon. This relationship is consistent with equilibrium isotope effects observed between elemental sulfur and sulfide in equilibrium with polysulfides (S_n^{2-}) (Amrani et al., 2006), and could reflect either abiotic speciation of ZVS at the redox interface, or intracellular equilibrium isotope effects associated with sulfide oxidation by anoxygenic phototrophs (Zerkle et al., 2009). No ZVS passes through a 0.45 µm filter at 20.5 m, demonstrating that ZVS at the chemocline is in particulate form (Fig. 4), either stored intracellularly or associated with organic matter in the form of biological sulfur globules (e.g., Kleinjan et al., 2005). In April, ZVS is only ~1‰ enriched in ^{34}S over sulfide at the chemocline, likely reflecting a dampening in the expression of these isotope effects due to very fast turnover of sulfide by a more productive phototroph community. A similar metabolic control on fractionation has been demonstrated for sulfate-reducing bacteria, which produce smaller fractionations at higher rates of sulfate reduction, when entry of sulfate into the cell becomes rate-limiting (see Canfield, 2001b, for a detailed discussion).

In contrast to the similar $\delta^{34}S$ values of ZVS samples from the chemocline in October, the $\Delta^{33}S$ values of these samples are dramatically different (Table 1 and Fig. 5). The $\Delta^{33}S$ of ZVS from the top of the chemocline is ~0.1‰ less than the ZVS sampled below, corresponding to a maximum in turbidity (indicating the most dense phototroph community). A similar difference in the $\Delta^{33}S$ has been shown to occur between the first-formed ZVS product from phototrophic sulfide oxidation and the residual ZVS reactant during phototrophic oxidation of ZVS to sulfate by the green sulfur bacterium *Chlorobium* (syn. *Chlorobaculum*) *tepidum* (Zerkle et al., 2009). This change in $\Delta^{33}S$ may indicate that further phototrophic oxidation of ZVS is occurring at the top of the FGL chemocline. Many anoxygenic phototrophs will oxidize ZVS when sulfide is limiting (Pfennig, 1975), and these organisms tend to be sulfide-limited in the top of chemocline communities in stratified sys-

Table 1
Sulfur isotope values of sulfide (AVS), zero-valent sulfur (ZVS), and sulfate in the water column of Green Lake, normalized to VCDT (in ‰). σ values are standard deviations on individual analyses (for $n \geq 3$ runs per sample). Data are plotted in Fig. 5.

S species	Depth (m)	$\delta^{34}S$	σ	$\Delta^{33}S$	σ	$\Delta^{36}S$	σ
April–May, 2009							
AVS	20.5	−28.49	0.007	0.144	0.010	−1.522	0.170
AVS	21	−29.47	0.005	0.151	0.013	−1.524	0.147
AVS	21.5	−30.99	0.003	0.143	0.009	−1.565	0.086
AVS	22	−29.35	0.003	0.128	0.007	−1.539	0.090
AVS	23	−30.66	0.006	0.132	0.012	−1.569	0.083
AVS	25	−29.81	0.005	0.141	0.003	−1.548	0.121
AVS	26.5	−29.52	0.005	0.133	0.003	−1.526	0.011
AVS	28	−29.21	0.003	0.147	0.007	−1.533	0.053
AVS	30	−28.95	0.005	0.142	0.016	−1.630	0.081
AVS	33	−28.15	0.009	0.144	0.017	−1.627	0.092
AVS	37	−27.29	0.006	0.147	0.013	−1.552	0.100
AVS	40	−26.02	0.007	0.144	0.002	−1.654	0.129
AVS	43	−24.27	0.005	0.148	0.014	−1.500	0.152
AVS	47	−24.14	0.004	0.148	0.005	−1.528	0.131
AVS	49	−24.21	0.004	0.162	0.009	−1.493	0.069
ZVS	20	−26.94	0.008	0.126	0.007	−1.356	0.147
ZVS	20.6	−28.06	0.018	0.115	0.012	−1.520	0.071
Sulfate	15	24.60	0.011	−0.003	0.012	0.030	0.135
Sulfate	20	24.87	0.006	0.019	0.007	0.043	0.071
Sulfate	20.5	25.12	0.005	0.007	0.014	−0.131	0.106
Sulfate	21	24.93	0.006	0.010	0.012	0.065	0.043
Sulfate	21.5	26.70	0.004	0.018	0.002	−0.087	0.073
Sulfate	25	28.41	0.004	0.012	0.014	−0.058	0.119
Sulfate	30	29.21	0.007	0.013	0.009	−0.068	0.121
Sulfate	43	29.11	0.004	0.070	0.007	−0.394	0.151
Sulfate	49	30.97	0.012	0.034	0.011	−0.232	0.018
October, 2008							
AVS	20.1	−26.12	0.006	0.150	0.007	−1.609	0.067
AVS	20.5	−26.41	0.012	0.088	0.014	−1.207	0.255
AVS	20.9	−28.68	0.004	0.134	0.003	−1.558	0.013
AVS	22.1	−30.25	0.005	0.139	0.009	−1.513	0.115
AVS	23.0	−30.03	0.004	0.148	0.006	−1.543	0.141
AVS	25.0	−29.35	0.008	0.145	0.010	−1.701	0.032
AVS	26.5	−29.48	0.007	0.141	0.015	−1.688	0.083
AVS	28.0	−29.14	0.006	0.137	0.008	−1.756	0.112
AVS	30.0	−28.73	0.006	0.142	0.014	−1.510	0.109
AVS	33.1	−28.05	0.011	0.139	0.017	−1.524	0.127
AVS	40.0	−26.02	0.011	0.140	0.011	−1.547	0.099
AVS	44.1	−24.97	0.009	0.146	0.011	−1.636	0.053
ZVS	20	−19.66	0.016	0.017	0.014	−0.127	0.519
ZVS	20.5	−19.60	0.018	0.120	0.015	0.257	0.382
Sulfate	5.2	21.85	0.007	0.029	0.009	0.053	0.116
Sulfate	15.0	24.25	0.010	−0.001	0.013	0.032	0.162
Sulfate	19.0	24.17	0.005	−0.003	0.005	0.080	0.092
Sulfate	19.5	24.01	0.002	0.005	0.005	0.105	0.064
Sulfate	20.1	24.29	0.005	−0.006	0.008	0.030	0.067
Sulfate	20.5	24.84	0.003	0.005	0.010	0.171	0.074
Sulfate	20.9	25.09	0.007	0.015	0.013	0.126	0.115
Sulfate	22.1	25.09	0.007	0.015	0.013	0.126	0.115
Sulfate	23.0	27.08	0.007	0.030	0.012	0.012	0.087
Sulfate	25.0	28.22	0.003	0.017	0.004	0.042	0.052
Sulfate	26.5	27.73	0.005	0.026	0.003	0.013	0.082
Sulfate	28.0	28.59	0.006	0.014	0.004	−0.042	0.121
Sulfate	30.0	28.59	0.006	0.014	0.004	−0.042	0.121
Sulfate	33.1	28.54	0.004	0.045	0.010	0.042	0.433
Sulfate	37.1	29.80	0.004	0.039	0.003	0.015	0.116
Sulfate	40.0	30.75	0.012	0.046	0.014	0.070	0.055
Sulfate	44.1	31.38	0.011	0.054	0.010	0.050	0.087

(*continued on next page*)

Table 1 (*continued*)

S species	Depth (m)	$\delta^{34}S$	σ	$\Delta^{33}S$	σ	$\Delta^{36}S$	σ
Sulfate	47.0	32.17	0.006	0.038	0.010	0.099	0.088
November, 2007							
AVS	22.5	−29.84	0.009	0.130	0.003		
AVS	25	−29.19	0.002	0.134	0.005		
AVS	30	−28.60	0.008	0.142	0.016		
AVS	47	−24.67	0.011	0.114	0.015		
Sulfate	5	23.91	0.014	−0.018	0.005		
Sulfate	19.8	25.06	0.012	−0.010	0.021		
Sulfate	20.8	25.59	0.010	0.006	0.016		
Sulfate	22.5	26.45	0.007	−0.011	0.019		
Sulfate	25	26.74	0.008	0.013	0.013		
Sulfate	30	30.51	0.009	0.040	0.008		
Sulfate	47	30.58	0.011	0.037	0.015		

tems (e.g., Guerrero et al., 1985). Therefore, we would expect ZVS oxidation to be occurring at this horizon, but see evidence for this process only in the minor isotopes. In April, the $\Delta^{33}S$ signature disappears, again presumably due to more efficient recycling of sulfide and ZVS.

In summary, the isotope values of sulfur species at the chemocline indicate that several processes are contributing to sulfide oxidation, and the importance of these processes fluctuates seasonally. Reaction of sulfide with oxygen dominates the oxidation processes in the fall when the phototroph community is recovering from lowered light levels after a whiting event. In the spring before a whiting event, the anoxygenic phototroph community is more pronounced, and contributes a greater proportion of sulfide oxidation. There may also be times during which phototrophic S-oxidation dominates sulfide oxidation at the chemocline, as seen in Fry (1986; sampling season not reported). While the S isotope values of sulfide at the chemocline reflect multiple oxidation processes, the values of ZVS appear to reflect production and reoxidation by phototrophic S-oxidation. The change in fractionations between sulfide and ZVS decrease with enhanced phototrophic oxidation in the spring, suggesting that the fractionations respond to metabolic rates in a manner similar to sulfate reducers.

5.2. Sulfur cycling in the monimolimnion

We and others have measured very large fractionations in $\delta^{34}S$ between sulfate and sulfide in the FGL monimolimnion (>48‰). These fractionations indicate that sulfate reduction in the lake is producing larger fractionations than those measured in laboratory experiments, and/or that oxidative recycling of sulfide is contributing to the isotopic signal. We can further constrain the contribution of sulfur metabolisms to the sulfur cycle in the lake by examining the trends in $\delta^{34}S$ and minor S isotope values of sulfur species in the monimolimnion.

5.2.1. Trends in sulfate S isotopes

Sulfate S isotope values show a fairly wide range in the surface waters ($\delta^{34}S$ from +22‰ to +25‰), then increase in both $\delta^{34}S$ and $\Delta^{33}S$ with depth in the monimolimnion (Fig. 5). Deevey et al. (1963) measured a $\delta^{34}S$ value of +24.7‰ for sulfate in the primary surface inlet of the lake. The lighter $\delta^{34}S$ values we measure at around 5 m (Table 1) could reflect mixing with sulfate delivered by precipitation or an additional surface source. S isotope values for gypsum from the Vernon Shale have not been published; however, the sulfate S isotope values at and below the chemocline suggest a heavier $\delta^{34}S$ for the subsurface sulfate source. The increase in sulfate S isotopes with depth in the monimolimnion could reflect a difference in the isotopic composition of sulfate input into the deep water, or alternatively it could reflect changes in water column S cycle processes that consume sulfate and recycle reduced sulfur. Torgersen et al. (1981) hypothesized the presence of a secondary chemocline in the FGL water column at around 32.5 m, potentially associated with a secondary source of groundwater input at this depth. Since we have not directly sampled the groundwater inputs we cannot completely disregard a change in the composition of the source sulfate associated with a secondary input. However, both sources would derive their sulfate from dissolution of gypsum in the surrounding Vernon Shale, and should therefore have a uniform isotopic composition.

A simple scenario capable of producing this trend in sulfate S isotopes via changes in the sulfur cycle would be a reservoir effect associated with irreversible consumption of sulfate at depth. A Rayleigh-type model can be used to describe this effect in a closed system, where sulfate consumption proceeds via a single unidirectional process (i.e., sulfate reduction) with a constant fractionation factor, and no isotope exchange occurs between residual sulfate and product sulfide (Mariotti et al., 1981). We calculated the isotopic composition (in $\delta^{34}S$ and $\Delta^{33}S$) of residual sulfate and accumulated sulfide in FGL produced under such a scenario, using a fractionation in $\delta^{34}S$ based on the measured values ($^{34}\alpha = 0.945$) and a range of $^{33}\lambda$ values approximating equilibrium (0.515) and sulfate reduction (0.512–0.513) processes. With this model we can reproduce the general trends in $\delta^{34}S$ and $\Delta^{33}S$ in both sulfate and sulfide utilizing a lambda value of 0.513; however, this model requires that greater than 20% of sulfate is reduced to sulfide during sulfate reduction. If this scenario is correct we would expect to see the buildup of 2.4 to greater than 3.2 mM sulfide in the deep waters, which is significantly larger than the 1.5–1.8 mM sulfide we measure. Conservation of sulfur mass in the monimolimnion (sulfide + sulfate + S-intermediates)

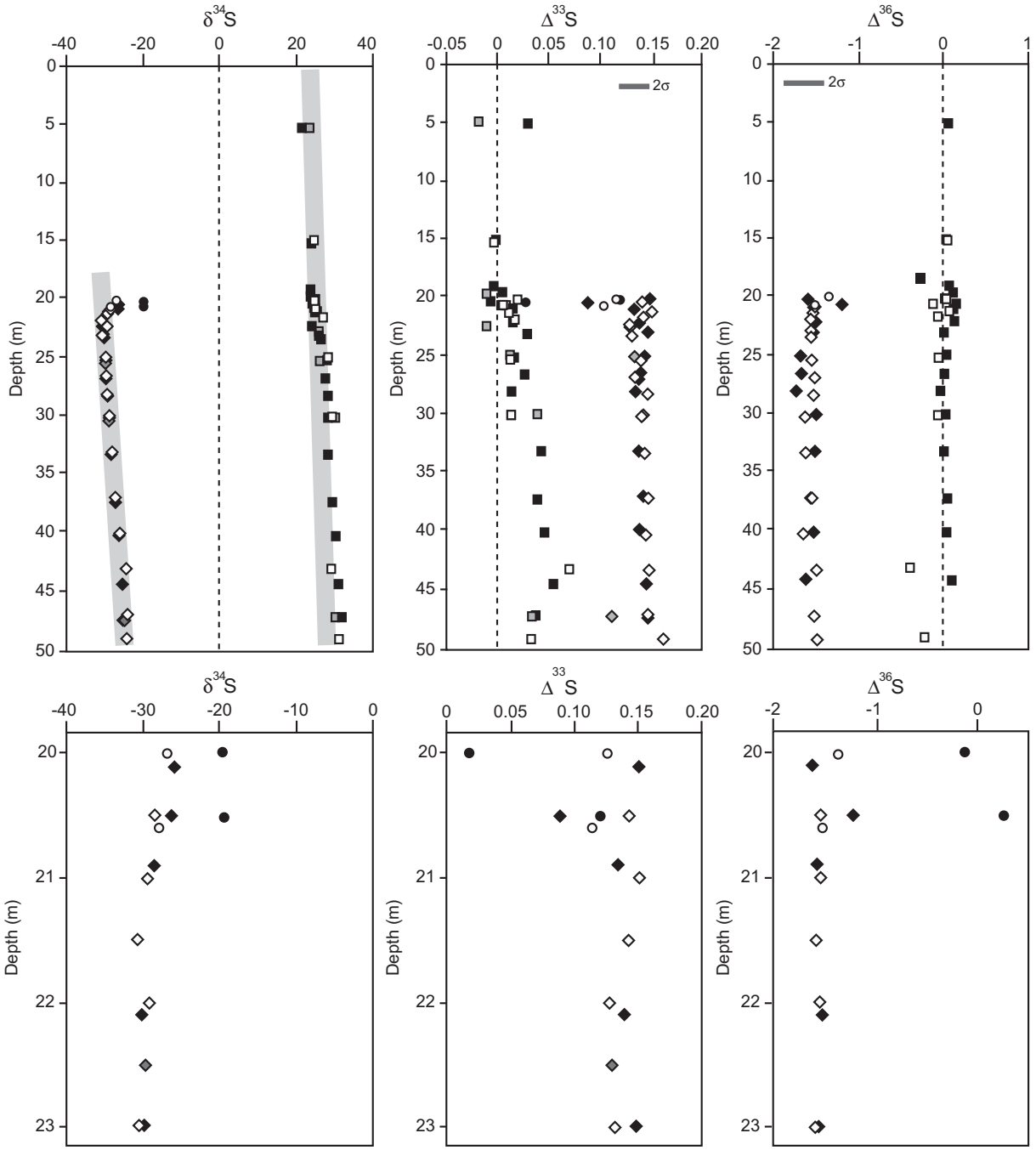

Fig. 5. $\delta^{34}S$, $\Delta^{33}S$, and $\Delta^{36}S$ for sulfide (diamonds), sulfate (squares), and ZVS (circles) in the FGL water column. Gray symbols are from November, 2007, black symbols are from October, 2008, and white symbols are from April, 2009. The gray bars for $\delta^{34}S$ indicate the range of values presented in Deevey et al. (1963) (sampled in June) and Fry (1986) (sampling season not reported). Bottom panels provide a closer look at sulfide and ZVS isotope values across the chemocline, from 20 to 23 m. Data are given in Table 1.

suggests that no significant amount of sulfur is lost from the water column (e.g., via burial of sulfide as pyrite in sediments). Therefore, the concentration of sulfide in the deep waters is insufficient to support a single-step removal process for sulfate in the deep waters. Instead, a more complex sulfur cycle, including multiple removal processes for sulfate and/or recycling of sulfide in the water column, is required to produce the measured isotope values.

5.2.2. Depth-derived model of sulfide

We examined more complex scenarios for the FGL sulfur cycle by constructing a one-dimensional depth-derived model of sulfide in the monimolimnion, considering physical as well as biogeochemical processes. In this model, we include diffusion, advection, sulfate reduction (SR), sulfur compound disproportionation (SD), and sulfide oxidation (SO) processes (Table 2). We utilized this model to fit the

Table 2
Inputs for the one-dimensional depth-derived sulfide models. Diffusion rates are in $m^2\ day^{-1}$, upwelling rates are in $m\ day^{-1}$, and metabolic rates are in $mmol\ m^{-3}\ day^{-1}$. SO is sulfide oxidation, SR is sulfate reduction, and SD is sulfur compound disproportionation. Ranges are values used for a best fit of the mean sulfide data, and best fits for the mean ± estimated error. Model A was run with sulfate reduction fractionations set to the maximum measured in laboratory cultures (48‰), and does not fit the data (Fig. 6). Model B was run with sulfate reduction fractionations set to a best fit of the data, and requires fractionations outside those possible for the SR metabolism (Fig. 7). Model C was run including disproportionation, and can fit the data with reasonable (although still large) SR fractionations (Fig. 6 and 7).

Model/process	Depth (m)	Rate	$^{34}\alpha$	$^{33}\lambda$
(A) Transport + SO + SR (set to 48‰)				
Diffusion	20–50	0.0864	1.000	0.5150
Upwelling	20–50	0.014	1.000	0.5150
SO	20–21	0.5	1.005	0.5150
SR	20–25	2.5–3.0	0.952	0.5130
SR	26–44	0.07–0.1	0.952	0.5130
SR	45–50	0.4–0.8	0.952	0.5130
(B) Transport + SO + SR (variable)				
Diffusion	20–50	0.0864	1.000	0.5150
Upwelling	20–50	0.014	1.000	0.5150
SO	20–21	0.5	1.005	0.5150
SR	20–25	2.5–3.0	0.944	0.5130
SR	26–44	0.07–0.1	0.928–0.932	0.5135
SR	45–50	0.4–0.8	0.945	0.5130
(C) Transport + SO + SR (variable) + SD				
Diffusion	20–50	0.0864	1.000	0.5150
Upwelling	20–50	0.014	1.000	0.5150
SO	20–21	0.5	1.005	0.5150
SR	20–25	1.0–1.4	0.950–0.952	0.5131
SR	26–44	0.07–0.1	0.935–0.938	0.5140
SR	45–50	0.3–0.8	0.945	0.5130
SD	20–25	0.5	0.985	0.5120
SD	26–37	0.04–0.05	0.985	0.5120

general trends in sulfide in the monimolimnion (the concentration profiles, and the large fractionations between sulfide and sulfate). Sulfide oxidation is concentrated in the upper few meters of the monimolimnion, and as such is difficult to examine within the scale of this model (refer to Section 5). We use the following equation to calculate sulfide concentrations:

$$\frac{\partial C}{\partial t} + D\frac{\partial^2 C}{\partial z^2} - U\frac{\partial C}{\partial z} + q_{SR} + q_{SD} - q_{SO} = 0 \quad (9)$$

where C is the concentration, D is the vertical diffusivity, U is the upwelling velocity, and q terms are the various metabolic rates. We also calculate sulfide $\delta^{34}S$ and $\delta^{33}S$ using the equation:

$$\frac{\partial \delta^{3X}S}{\partial t} = \left(\sum_{i=1}^{n} F_i \cdot \delta^{3X}S_i - \delta^{3X}S\frac{\partial C}{\partial t}\right) \Big/ C, \quad (10)$$

where F_i refers to the different sulfur mass fluxes (e.g., via diffusion, upwelling, sulfate reduction, etc.; Table 2). We solved the system of equations using a FTCS (forward in time centered in space) finite difference approximation, with a time step of 1 day and a spatial step of 1 m. Boundary conditions were set at 1.5–1.8 mM sulfide at the bottom boundary (to reflect the mean sulfide concentration near the sediment–water interface ± estimated error), with an isotopic composition of $\delta^{34}S = -24.6‰$ and $\Delta^{33}S = 0.15‰$, and 0 mM sulfide at the top boundary. Initial conditions were set at 0 mM sulfide. Sulfate concentration was held constant (i.e., non-limiting) with depth. As discussed above, we have no constraints on the isotopic composition of sulfate entering the monimolimnion, so we used the measured sulfate isotope values with depth as the starting value for sulfate reduction. We used vertical diffusivity and upwelling velocities derived for the FGL monimolimnion by Torgersen et al. (1981). We assumed that the diffusivity and upwelling rates are constant and independent of depth, and that no fractionation is associated with either of these transport processes. Sulfide oxidation and associated fractionation was only calculated in the top boxes of the model (at the chemocline) where the majority of the oxidation is occurring (e.g., Mandernack and Tebo, 1999). We used a sulfide oxidation rate similar to values measured in the chemoclines of other stratified systems (from Mandernack and Tebo, 1999; Table 2), and assumed a fractionation of +5‰ for inorganic sulfide oxidation. Below this, the isotopic value of S-intermediates (as the substrate for disproportionation) was set to that of the coexisting sulfide, assuming oxidative production associated with very small isotope effects compared to sulfate reduction and sulfur disproportionation (see Section 5). The model reaches steady state from zero after about 20 years.

Sensitivity tests showed that the modeled sulfide concentration profile is most sensitive to diffusivity, rates of sulfate reduction and sulfur disproportionation, and the bottom boundary condition (sulfide input). The sulfide profile is only significantly affected by upwelling rates or oxidation rates at orders of magnitude higher values than estimated for this system. The $\delta^{34}S$ profile is primarily sensitive to the rates and alpha values used for sulfate reduction (and sulfur compound disproportionation). It is also fairly sensitive to the $\delta^{34}S$ used for input sulfide and coexisting sulfate, which were constrained by the data. The $\Delta^{33}S$ profile is similarly very sensitive to the alpha and lambda values used for sulfate reduction, and to the $\Delta^{33}S$ of the input sulfide and sulfate (also constrained by data).

All models included transport processes (diffusion and advection), sulfide oxidation, and sulfate reduction (Table 2). We varied the sulfate reduction rates with depth to fit the sulfide concentration profile, first for the mean sulfide concentrations, then for the sulfide concentrations ± estimated errors, to produce a range in SR rates and fractionations. Depths were binned according to reaction zones at the chemocline (20–25 m), the sediment–water interface (45–50 m) and the rest of the monimolimnion (26–44 m). We can fit the range of measured sulfide concentrations with high rates of sulfate reduction at the top of the monimolimnion (2.5–3 $mmol\ m^{-3}\ day^{-1}$), lower sulfate reduction rates in the middle of the monimolimnion (0.07–0.1 $mmol\ m^{-3}\ day^{-1}$), and moderate rates of sulfate reduction at the bottom of the monimolimnion (0.4–0.8 $mmol\ m^{-3}\ day^{-1}$) (Table 2). These sulfate reduction

rates are within the range of values calculated for other anoxic water bodies (e.g., Overmann et al., 1996), but higher than that estimated for FGL by Torgersen et al. (1981) based on calculated sulfide fluxes (0.005 mmol m^{-2} day^{-1}).

In the first model (Table 2, model A) we set the $^{34}\alpha$ value for sulfate reduction constant at 0.952, representing the maximum fractionation measured in laboratory experiments with sulfate-reducing prokaryotes (48‰; Kaplan and Rittenberg, 1964; Canfield, 2001a; Detmers et al., 2001; Habicht and Canfield, 2001). This model demonstrates that the maximum experimental fractionation for SR is insufficient to fit the data for $\delta^{34}S$ (Fig. 6, solid line). We ran a second model with variable values of $^{34}\alpha$ and $^{33}\lambda$ for SR, to determine what fractionations are required to fit the isotope data without disproportionation (Table 2, model B). With this model we can only fit the measured $\delta^{34}S$ and $\Delta^{33}S$ values if we utilize extremely large fractionations in the middle of the monimolimnion, from 68‰ to 72‰, with $^{33}\lambda$ values of 0.513–0.5135. These fractionations for SR are impossible based on our current knowledge of the sulfate reduction metabolism, plotting well outside the range of possible fractionations in $\delta^{34}S$ and $\Delta^{33}S$ calculated by Farquhar et al. (2007) based on the SR metabolic models of Brunner and Bernasconi (2005) (Fig. 7, black symbols). In the final model, we included sulfur compound disproportionation, utilizing constant $^{34}\alpha$ and $^{33}\lambda$ values for disproportionation (0.985 and 0.512, respectively), and adjusting sulfate reduction parameters to fit the measured data (Table 2, model C). We used disproportionation rates of 0.04–0.5 mmol m^{-3} day^{-1}, which are consistent with measured rates of sulfur disproportionation in pure and enrichment cultures (Böttcher and Thamdrup, 2001; Böttcher et al., 2001, 2005) and the high density of cells in the FGL chemocline (10^7 cells/ml; Thompson et al., 1990). This model is the only model that can fit the measured data using reasonable values for SR fractionations (Fig. 6, dotted line). The required SR fractionations are still larger than

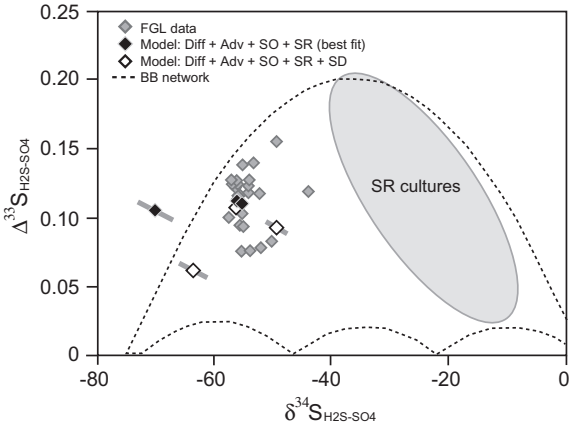

Fig. 7. Comparison of fractionations from this study with the field of possible $\delta^{34}S$ and $\Delta^{33}S$ values calculated by Farquhar et al. (2007) for the Brunner and Bernasconi (2005) model of the sulfate reduction metabolism (dotted line). Gray symbols are fractionations between sulfide and sulfate measured in the GL water column. These values plot within the field but near its limits. Black symbols are the fractionations for SR that are required to fit the data in a model without sulfur compound disproportionation (Table 2, model B), and include fractionations outside the range of possible $\delta^{34}S$ and $\Delta^{33}S$ values for the sulfate reduction metabolism. Empty symbols are the fractionations for SR that fit a model including sulfur compound disproportionation (Table 2, model C). These fractionations plot within the range of possible values, but are still much larger than those measured in culture experiments with sulfate-reducing prokaryotes (shown as gray area; data from Farquhar et al., 2003; Johnston et al., 2005a, 2007). The gray bars on the model values represent the range of fractionations required to fit models for the mean sulfide concentrations ± estimated error.

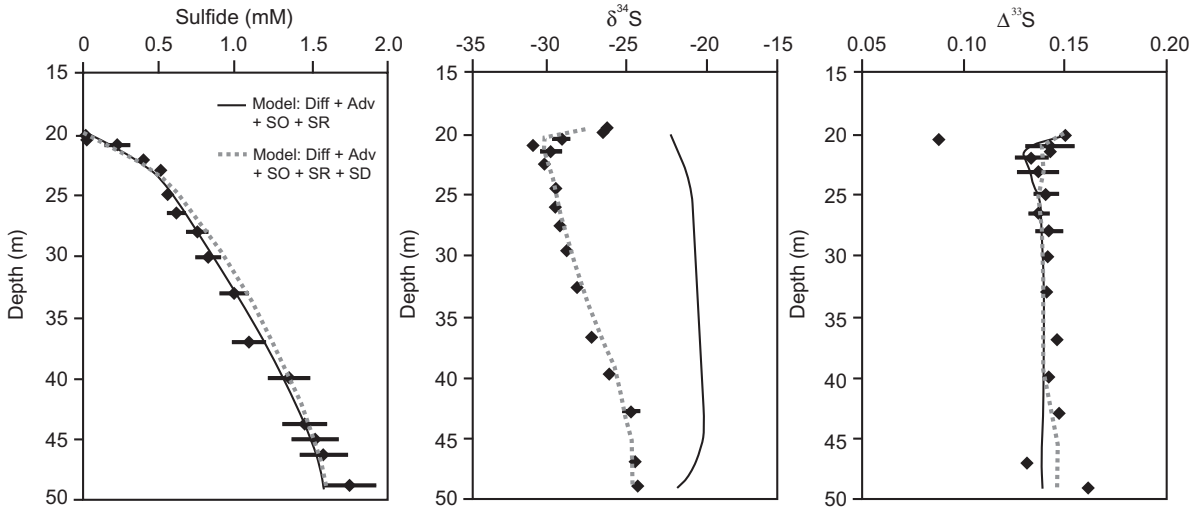

Fig. 6. Depth-derived models of sulfide concentrations and isotopes ($\delta^{34}S$ and $\Delta^{33}S$) in the FGL monimolimnion. Symbols are mean values for data from all three sample sets, with error bars representing the standard deviation between sets (isotopes) or the estimated analytical error (sulfide). The solid line is the model including transport + sulfide oxidation + sulfate reduction at a fractionation of 48‰ (Table 2, model A). The dotted line is the best fit model including transport + sulfide oxidation + sulfate reduction (at a variable fractionation) + sulfur compound disproportionation (Table 2, model C).

those measured in laboratory experiments; however, they plot within the range of possible $\delta^{34}S$ and $\Delta^{33}S$ values for the SR metabolism (Fig. 7, white symbols). The model therefore requires both sulfur compound disproportionation and large SR fractionations to reproduce the measured isotope trends in the FGL water column.

We discuss further lines of evidence for disproportionation and its significance in the following section. The modeled patterns in SR fractionations required to fit the data provide some insight into the controls on sulfate reduction in the FGL monimolimnion as well. These SR fractionations vary with depth and are inversely proportional to sulfate reduction rates. SR fractionations respond to environmental variables such as temperature, sulfate availability, and electron donor supply (Harrison and Thode, 1958; Kaplan and Rittenberg, 1964; Habicht et al., 2002). Temperature remains constant with depth in the FGL monimolimnion (Fig. 2), and sulfate concentrations are uniformly high, allowing the expression of large fractionations (Habicht et al., 2002). Experiments with sulfate reducers utilizing various organic electron donors has shown that the extent of fractionation responds to the specific rates of sulfate reduction (rates/cell) (Harrison and Thode, 1958; Kaplan and Rittenberg, 1964; Kemp and Thode, 1968; Chambers et al., 1975), as we see with water column sulfate reduction rates in the model. This trend suggests that the change in fractionations with depth predicted by the model could be related to changes in the availability or quality of organic matter. Primary production at the chemocline provides an abundant source of organic matter to support high rates of sulfate reduction at and just below this interface. The amount and quality of organic matter should decrease with depth below the chemocline, as the most "labile" organic compounds are preferentially consumed, leading to lower rates of sulfate reduction and correspondingly higher fractionations lower in the water column. In this scenario, the moderately high sulfate reduction rates and fractionations at the "bottom" of the modeled lake might then reflect sulfate reduction processes in the sediments, where the residual organic matter is concentrated and sulfate reduction rates in some cases can be higher than in the water column (e.g., Sørensen and Canfield, 2004). The $\delta^{34}S$ values of sulfate and sulfide in the deep part of the basin (43–49 m) are identical to that of the pore-water sulfate and acid-volatile sulfur in the top of the sediments (Riccardi, 2007), supporting a sediment source without the necessity for additional sulfate reduction in the bottom part of the water column. We tested this scenario by setting sulfate reduction rates constant at 0.1 mmol m^{-3} day^{-1} from 26 to 50 m, and increasing the bottom boundary condition (reflecting a greater sulfide input from the sediments), and found we can still fit the sulfide concentration and isotopic data in the deepest boxes reasonably well (not shown). We therefore conclude that high sulfate concentrations and organic matter distribution are responsible for sulfate reduction rates and associated large fractionations in the FGL water column.

5.2.3. Evidence for sulfur compound disproportionation

The model we present above requires sulfur compound disproportionation to produce the measured isotope trends in the FGL water column. Further lines of evidence, both geochemical and biological, support a role for disproportionation in the sulfur cycle of this system. Specifically, geochemical profiles of S compounds in the lake reflect the availability and intense recycling of intermediate sulfur compounds utilized in disproportionation. Thiosulfate, sulfite, and ZVS are all used as substrates for SD (Bak and Cypionka, 1987; Bak and Pfennig, 1987; Kramer and Cypionka, 1989; Thamdrup et al., 1993). Profiles of sulfite and thiosulfate in FGL (Fig. 3) lack the pronounced peak at the redox interface that is common in other stratified aqueous systems (Zopfi et al., 2001; Li et al., 2008), indicating very fast turnover of these compounds at the chemocline. Particulate extracellular ZVS provides another substrate for disproportionation just below the chemocline (at 22 m, Fig. 4). Furthermore, organisms related to known disproportionators have been identified at various depths in the FGL water column (*Desulfocapsa* sp., Meyer, 2008).

Thamdrup et al. (1993) calculated that disproportionation of ZVS is thermodynamically favorable only at very low activities of sulfide (<1 μM), but these researchers also demonstrated that disproportionation can sustain bacterial growth at higher sulfide concentrations in the presence of a sulfide scavenger, such as FeOOH or Mn-oxides. The cultures in this study continued to accumulate sulfide to concentrations of >1 mM even after the metal oxides were depleted (Thamdrup et al., 1993). Given these constraints, disproportionation of ZVS could proceed unimpeded at the very low sulfide levels presumably sustained at the top of the FGL chemocline. However, even at 22 m where extracellular particulate ZVS is an available substrate, sulfide concentrations reach up to 370 μM (Figs. 3 and 4). Disproportionation of ZVS could still occur at this depth if coupled to Fe or Mn reduction, as in the Thamdrup et al. study. Both amorphous and crystalline Fe-oxides are present in the top 0.5 cm of FGL sediments (Suits and Wilkin, 1998), indicating surface influx and settling of FeOOH through the water column, providing such an electron sink for SD even at the depths indicated by our model (>35 m).

A second option would be a biological sulfide sink for disproportionation, specifically involving an association with sulfide oxidizing phototrophs. Such a synergistic relationship has been suggested for meromictic Lake Cadagno, in Switzerland, where researchers identified aggregates of the disproportionator *Desulfocapsa* sp. and the phototrophic sulfide oxidizer *Lamprocystis* sp. (Peduzzi et al., 2003a,b; Tonolla et al., 2003). The spatial coupling and complementary metabolisms of these organisms led the researchers to postulate a source–sink relationship for sulfide. The aggregates form up to 45% of the microbial community at the Lake Cadagno chemocline, suggesting an important role for these organisms in sulfur cycling at the redox interface. Similar aggregates have been observed in FGL, and clones related to both genera identified in Lake Cadagno have been retrieved from samples at and below the chemocline (at 20.5 m and 25 m depth; Meyer, 2008). This type of relationship is therefore likely to be occurring in FGL and, if widespread, could have important implications for the distribution of disproportionation in natural systems.

6. CONCLUSIONS

A comparison of our S isotope data with results of previous studies indicates that FGL is an appropriate natural laboratory for understanding steady-state sulfur cycling in stratified euxinic systems with intermediate sulfate concentrations (e.g., ancient oceans). The sulfur cycle of FGL is remarkably stable over long periods of time, and is not markedly affected by seasonal changes in light availability or organic matter delivery, with the exception of at the chemocline. The biogeochemical processes contributing to sulfur cycling, however, appear to be spatially heterogeneous with depth in the FGL water column, and are reflected in the isotopic composition of sulfur species.

Sulfide is enriched in ^{34}S across the redox interface by sulfide oxidation via reaction with O_2, in spite of the dense population of phototrophic S-oxidizing organisms that inhabit the chemocline. Very little evidence for this abiotic oxidation is seen in the concentrations or isotopes of product sulfur species, e.g., thiosulfate, sulfite, or zero-valent sulfur, suggesting very fast turnover of S-intermediates by oxidation and/or disproportionation processes. The isotopic enrichment in sulfide across the chemocline is less pronounced in the spring than in the fall, consistent with a greater contribution from phototrophic S-oxidation reactions under higher light availability before a whiting event. Size distribution and isotopic values of ZVS in the chemocline in October reflect production and reoxidation by phototrophic processes, including intercellular isotope exchange between S^0, polysulfides, and sulfide, and further oxidation of ZVS to sulfate. Smaller fractionations are measured between sulfide and zero-valent sulfur in April, suggesting a metabolic rate control on the extent of fractionation similar to that seen in sulfate-reducing prokaryotes.

In the deep waters of FGL, the high sulfate concentration (16 mM) buffers against large changes in the S isotopes of sulfate (and sulfide) while allowing for very large fractionations during sulfate reduction. Numerical models of sulfide $\delta^{34}S$ and $\Delta^{33}S$ require that the fractionations for sulfate reduction are much larger than those measured in laboratory cultures, even in models including additional fractionation via oxidative recycling. The relationship between fractionations and sulfate reduction rates and their distribution with depth suggest that these fractionations are related to changes in the availability or quality of organic matter in the water column. The isotopic composition of sulfide and sulfate near the lake bottom, on the other hand, seems primarily to reflect sulfate reduction processes in the sediments. The numerical models coupled with profiles of intermediate sulfur compounds and the microbiology of the lake support a role for disproportionation in the FGL sulfur cycle, particularly at the chemocline. The occurrence of disproportionation at high sulfide concentrations deeper in the water column requires a close association with a sulfide sink, either abiotic or biological, highlighting some interesting questions about the distribution of disproportionation in natural systems and providing a target for future research.

In summary, the results of this study indicate that FGL harbors a complex sulfur cycle, with multiple processes contributing to sulfide oxidation at the chemocline and sulfur compound formation in the deep waters. Some of these processes are evident from the $\delta^{34}S$ values (e.g., oxidation of sulfide with O_2), but others are only inferred from minor isotope patterns (e.g., disproportionation and potentially ZVS oxidation). The inclusion of minor S isotopes in studies of sulfur compounds in this, and presumably other, natural systems facilitates the identification and quantification (to some extent) of these sulfur cycling processes.

ACKNOWLEDGMENTS

The authors would like to thank Z. Oliver, Y. Park, A. Masterson, and S.-T. Kim for assistance in the laboratory, and Z. Mansaray for assistance in the field. We also thank J. Dinman who kindly allowed us to use his HPLC. We would additionally like to thank the rangers and staff at Green Lakes State Park for providing access to the lake, boating equipment, and friendly assistance. This study greatly benefited from discussions with J. Macalady, K. Habicht, W. Gilhooly, J. Maresca, and a suite of researchers in the Department of Geosciences at Pennsylvania State University who have been utilizing FGL as a natural laboratory for many years. W. Gilhooly and two anonymous reviewers are thanked for thoughtful and constructive comments on the manuscript. This work was supported by funds from the NASA EXB program (to A.Z.), Marie Curie Outgoing International Fellowship SULFUTOPES number POIF-GA-2008-219586 and NSF Geobiology and Low Temperature Geochemistry Program Grant No. – 0843814 (to A.K.), and NSF EAR and NASA NAI programs (to J.F. and L.K.).

REFERENCES

Amrani A., Kamyshny, Jr., A., Lev O. and Aizenshtat Z. (2006) Sulfur stable isotope distribution of polysulfide anions in $(NH_4)_2S_n$ aqueous solution. *Inorg. Chem.* **45**, 1427–1429.

Bak F. and Cypionka H. (1987) A novel type of energy-metabolism involving fermentation of inorganic sulfur compounds. *Nature* **326**, 891–892.

Bak F. and Pfennig N. (1987) Chemolithotrophic growth of *Desulfovibrio sulfodismutans* sp. nov. by disproportionation of inorganic sulfur compounds. *Arch. Microbiol.* **147**, 184–189.

Böttcher M. E. and Thamdrup B. (2001) Anaerobic sulfide oxidation and stable isotope fractionation associated with bacterial sulfur disproportionation in the presence of MnO_2. *Geochim. Cosmochim. Acta* **65**, 1573–1581.

Böttcher M. E., Thamdrup B. and Vennemann T. W. (2001) Oxygen and sulfur isotope fractionation during anaerobic bacterial disproportionation of elemental sulfur. *Geochim. Cosmochim. Acta* **65**, 1601–1609.

Böttcher M. E., Thamdrup B., Gehre M. and Theune A. (2005) $^{34}S/^{32}S$ and $^{18}O/^{16}O$ fractionation during sulfur disproportionation by *Desulfobulbus propionicus*. *Geomicrobiol. J.* **22**, 219–226.

Brunner B. and Bernasconi S. M. (2005) A revised isotope fractionation model for dissimilatory sulfate reduction in sulfate reducing bacteria. *Geochim. Cosmochim. Acta* **69**, 4759–4771.

Brunskill G. J. (1969) Fayetteville Green Lake, New York: II. Precipitation and sedimentation of calcite in a meromictic lake with laminated sediments. *Limnol. Oceanogr.* **14**, 830–847.

Brunskill G. J. and Harriss R. C. (1969) Fayetteville Green Lake, New York: IV. Interstitial water chemistry of the sediments. *Limnol. Oceanogr.* **14**, 858–861.

Brunskill G. J. and Ludlam S. D. (1969) Fayetteville Green Lake, New York: I. Physical and chemical limnology. *Limnol. Oceanogr.* **14**, 817–829.

Brüchert V. (2004) Physiological and ecological aspects of sulfur isotope fractionation during bacterial sulfate reduction. In *Sulfur Biogeochemistry – Past and Present*, vol. 379 (eds. J. P. Amend, K. J. Edwards and T. W. Lyons), pp. 1–16. Sulfur Biogeochemistry – Past and Present. Geological Society of America Special Paper.

Canfield D. E. (2001a) Isotope fractionation by natural populations of sulfate-reducing bacteria. *Geochim. Cosmochim. Acta* **65**, 1117–1124.

Canfield D. E. (2001b) Biogeochemistry of sulfur isotopes. In *Stable Isotope Geochemistry, Reviews in Mineralogy and Geochemistry*, vol. 43, pp. 607–636.

Canfield D. E. and Teske A. (1996) Late Proterozoic rise in atmospheric oxygen concentration inferred from phylogenetic and sulphur-isotope studies. *Nature* **382**, 127–132.

Canfield D. E. and Thamdrup B. (1994) The production of ^{34}S-depleted sulfide during bacterial disproportionation of elemental sulfur. *Science* **266**, 1973–1975.

Canfield D. E., Farquhar J. and Zerkle A. L. (2010) High isotope fractionations during sulfate reduction in a low-sulfate euxinic ocean analog. *Geology* **38**, 415–418.

Canfield D. E., Thamdrup B. and Kristensen E. (2005) *Aquatic Geomicrobiology*. Elsevier.

Canfield D. E., Oleson C. A. and Cox R. P. (2006) Temperature and its control of isotopic fractionation by sulfate-reducing bacterium. *Geochim. Cosmochim. Acta* **70**, 548–561.

Chambers L. A., Trudinger P. A., Smith J. W. and Burns M. S. (1975) Fractionation of sulfur isotopes by continuous cultures of *Desulfovibrio desulfuricans*. *Can. J. Microbiol.* **21**, 1602–1607.

Cline J. D. (1969) Spectrophotometric determination of hydrogen sulfide in natural waters. *Limnol. Oceanogr.* **14**, 454–458.

Culver D. A. and Brunskill G. J. (1969) Fayetteville Green Lake, New York: V. Studies of primary production and zooplankton in a meromictic marl lake. *Limnol. Oceanogr.* **14**, 862–873.

Deevey, Jr., E. S., Nakai N. and Stuiver M. (1963) Fractionation of sulfur and carbon isotopes in a meromictic lake. *Science* **139**, 407–408.

Detmers J., Bruchert V., Habicht K. S. and Kuever J. (2001) Diversity of sulfur isotope fractionations by sulfate-reducing prokaryotes. *Appl. Environ. Microbiol.* **67**, 888–894.

Donahue M. A., Werne J. P., Meile C. and Lyons T. W. (2008) Modeling sulfur isotope fractionation and differential diffusion during sulfate reduction in sediments of the Cariaco Basin. *Geochim. Cosmochim. Acta* **72**, 2287–2297.

Farquhar J. and Wing B. A. (2003) Multiple sulfur isotopes and the evolution of the atmosphere. *Earth Planet. Sci. Lett.* **213**, 1–13.

Farquhar J., Johnston D. T., Wing B. A., Habicht K. S., Canfield D. E., Airieau S. and Thiemens M. H. (2003) Multiple sulphur isotopic interpretations of biosynthetic pathways: implications for biological signatures in the sulphur isotope record. *Geobiology* **1**, 27–36.

Farquhar J., Johnston D. T. and Wing B. A. (2007) Implications of conservation of mass effects on mass-dependent isotope fractionations: influence of network structure on sulfur isotope phase space of dissimilatory sulfate reduction. *Geochim. Cosmochim. Acta* **71**, 5862–5875.

Farquhar J., Canfield D. E., Masterson A., Bao H. and Johnston D. (2008) Sulfur and oxygen isotope study of sulfate reduction in experiments with natural populations from Faellestrand, Denmark. *Geochim. Cosmochim. Acta* **72**, 2805–2821.

Farquhar J., Canfield D. E., Zerkle A. L. and Habicht K. (2009) Isotope study of S-cycle of Lago di Cadagno. *Geochim. Cosmochim. Acta* **73**, A356.

Forrest J. and Newman L. (1977) Ag-110 microgram sulfate analysis for short time resolution of ambient levels of sulfur aerosol. *Anal. Chem.* **49**, 1579–1584.

Fry B., Gest H. and Hayes J. M. (1984) Isotope effects associated with the anaerobic oxidation of sulfide by the purple photosynthetic bacterium, *Chromatium vinosum*. *FEMS Microbiol. Lett.* **22**, 283–287.

Fry B. (1986) Sources of carbon and sulfur nutrition for consumers in three meromictic lakes of New York state. *Limnol. Oceanogr.* **31**, 79–88.

Fry B., Cox J., Gest H. and Hayes J. M. (1986) Discrimination between ^{34}S and ^{32}S during bacterial metabolism of inorganic sulfur-compounds. *J. Bacteriol.* **165**, 328–330.

Fry B., Ruf W., Gest H. and Hayes J. M. (1988) Sulfur isotope effects associated with oxidation of sulfide by O_2 in aqueous solution. *Chem. Geol.* **73**, 205–210.

Fry B., Jannasch H. W., Molyneaux S. J., Wirsen C. O., Muramoto J. A. and King S. (1991) Stable isotope studies of the carbon, nitrogen and sulfur cycles in the Black-Sea and the Cariaco Trench. *Deep Sea Res. Part A* **38**, S1003–S1019.

Gilhooly, III, W. P., Johnston D. T., Farquhar J., Severmann S. and Lyons T. W. (2009) Diverse pathways of sulfur cycling in the modern Black Sea captured in rare sulfur isotope signatures. *Geochim. Cosmochim. Acta* **73**, A435.

Goldhaber M. B. and Kaplan I. R. (1975) Controls and consequences of sulfate reduction rates in recent marine sediments. *Soil Sci.* **119**, 42–55.

Goldhaber M. B. and Kaplan I. R. (1980) Mechanisms of sulfur incorporation and isotope fractionation during early diagenesis in sediments of the Gulf of California. *Mar. Chem.* **9**, 95–143.

Granatelli L. (1959) Determination of microgram quantities of sulfur by reduction with Raney nickel. *Anal. Chem.* **31**, 434–436.

Gröger J., Franke J., Hamer K. and Schulz H. D. (2009) Quantitative recovery of elemental sulfur and improved selectivity in a chromium-reducible sulfur distillation. *Geostand. Geoanal. Res.* **33**, 17–27.

Guerrero R., Montesinos E., Pedrosalio C., Esteve I., Mas J., Vangemerden H., Hofman P. A. G. and Bakker J. F. (1985) Phototrophic sulfur bacteria in 2 Spanish lakes – vertical-distribution and limiting factors. *Limnol. Oceanogr.* **30**, 919–931.

Habicht K. S. and Canfield D. E. (2001) Isotope fractionation by sulfate-reducing natural populations and the isotopic composition of sulfide in marine sediments. *Geology* **29**, 555–558.

Habicht K. S., Canfield D. E. and Rethmeier J. (1998) Sulfur isotope fractionation during bacterial reduction and disproportionation of thiosulfate and sulfite. *Geochim. Cosmochim. Acta* **62**, 2585–2595.

Habicht K. S., Gade M., Thamdrup B., Berg P. and Canfield D. E. (2002) Calibration of sulfate levels in the Archean Ocean. *Science* **298**, 2372–2374.

Harrison A. G. and Thode H. G. (1958) Mechanism of the bacterial reduction of sulphate from isotope fractionation studies. *Trans. Faraday Soc.* **54**, 84–92.

Hulston J. R. and Thode H. G. (1965) Cosmic ray produced ^{36}S and ^{33}S in metallic phase of iron meteorites. *J. Geophys. Res.* **70**, 4435–4442.

Johnston D. T., Farquhar J., Wing B. A., Kaufman A., Canfield D. E. and Habicht K. S. (2005a) Multiple sulfur isotope fractionations in biological systems: a case study with sulfate reducers and sulfur disproportionators. *Am. J. Sci.* **305**, 645–660.

Johnston D. T., Wing B. A., Farquhar J., Kaufman A. J., Strauss H., Lyons T. W., Kah L. C. and Canfield D. E. (2005b) Active microbial sulfur disproportionation in the Mesoproterozoic. *Science* **310**, 1477–1479.

Johnston D. T., Poulton S. W., Fralick P. W., Wing B. A., Canfield D. E. and Farquhar J. (2006) Evolution of the oceanic sulfur cycle at the end of the Paleoproterozoic. *Geochim. Cosmochim. Acta* **70**, 5723–5739.

Johnston D. T., Farquhar J. and Canfield D. E. (2007) Sulfur isotope insights into microbial sulfate reduction: when microbes meet models. *Geochim. Cosmochim. Acta* **71**, 3929–3947.

Johnston D. T., Farquhar J., Habicht K. and Canfield D. E. (2008a) Sulphur isotopes and the search for life: strategies for identifying sulphur metabolisms in the rock record and beyond. *Geobiology* **6**, 425–435.

Johnston D. T., Farquhar J., Summons R. E., Shen Y., Kaufman A. J., Masterson A. L. and Canfield D. E. (2008b) Sulfur isotope biogeochemistry of the Proterozoic McArthur Basin. *Geochim. Cosmochim. Acta* **72**, 4278–4290.

Kamyshny, Jr., A., Borkenstein C. G. and Ferdelman T. G. (2009) Protocol for quantitative detection of elemental sulfur and polysulfide zero-valent sulfur distribution in natural aquatic samples. *Geostand. Geoanal. Res.* **33**, 415–435.

Kaplan I. R. and Rittenberg S. C. (1964) Microbiological fractionation of sulphur isotopes. *J. Gen. Microbiol.* **34**, 195–212.

Kemp A. L. W. and Thode H. G. (1968) Mechanism of bacterial reduction of sulphate and of sulphite from isotope fractionation studies. *Geochem. Cosmochim. Acta* **32**, 71–91.

Kleinjan W. E., de Keizer A. and Janssen A. J. H. (2005) Equilibrium of the reaction between dissolved sodium sulfide and biologically produced sulfur. *Colloids Surf. B* **43**, 228–237.

Kramer M. and Cypionka H. (1989) Sulfate formation via ATP sulfurylase in the thiosulfate-disproportionating and sulfite-disproportionating bacteria. *Arch. Microbiol.* **151**, 232–237.

Lein A. Y. and Ivanov M. V. (1990) Production of hydrogen-sulfide in shelf sediments and its balance in the Black Sea. *Microbiology* **59**, 637–642.

Li X. N., Taylor G. T., Astor Y. and Scranton M. I. (2008) Relationship of sulfur speciation to hydrographic conditions and chemoautotrophic production in the Cariaco Basin. *Mar. Chem.* **112**, 53–64.

Ludlam S. D. (1969) Fayetteville Green Lake, New York: III. The laminated sediments. *Limnol. Oceanogr.* **14**, 848–857.

Lyons T. W. (1997) Sulfur isotopic trends and pathways of iron sulfide formation in upper Holocene sediments of the anoxic Black Sea. *Geochim. Cosmochim. Acta* **61**, 3367–3382.

Lyons T. W., Werne J. P., Hollander D. J. and Murray R. W. (2003) Contrasting sulfur geochemistry and Fe/Al and Mo/Al ratios across the last oxic-to-anoxic transition in the Cariaco Basin, Venezuela. *Chem. Geol.* **195**, 131–157.

Mandernack K. W. and Tebo B. M. (1999) In situ measurements of microbial sulfide oxidation and CO_2 fixation at deep-sea hydrothermal vents and at the oxic–anoxic interface of Framvaren Fjord. *Mar. Chem.* **66**, 201–213.

Mandernack K. W., Krouse H. R. and Skei J. M. (2003) A stable sulfur and oxygen isotopic investigation of sulfur cycling in an anoxic marine basin, Framvaren Fjord, Norway. *Chem. Geol.* **195**, 181–200.

Mariotti A., Germon J. C., Hubert P., Kaiser P., Letolle R., Tardieux A. and Tardieux P. (1981) Experimental determination of nitrogen kinetic isotope fractionation – some principles – illustration for the denitrification and nitrification processes. *Plant Soil* **62**, 413–430.

Meyer K. M. (2008) Biogeochemistry of oceanic euxinia in earth history: numerical modeling and evaluation of biomarkers using modern analogs. Ph.D. dissertation, Department of Geosciences, The Pennsylvania State University, State College, Pennsylvania.

Muller E. A. (1967) Geologic setting of Green and Round Lakes near Fayetteville, New York. In *Some Aspects of Meromixis* (ed. D. F. Jackson). Department of Civil Engineering, Syracuse University, Syracuse, New York.

Muramoto J. A., Honjo S., Fry B., Hay B. J., Howarth R. W. and Cisne J. L. (1991) Sulfur, iron, and organic-carbon fluxes in the Black Sea – sulfur isotopic evidence for origin of sulfur fluxes. *Deep Sea Res. A* **38**, S1151–S1187.

Neretin L. N., Grinenko V. A. and Volkov I. I. (1996) Hydrogen sulfide isotopic composition in deep-water column of the Black Sea. *Dokl. Akad. Nauk* **349**, 542–545.

Neretin L. N., Böttcher M. E. and Grinenko V. A. (2003) Sulfur isotope geochemistry of the Black Sea water column. *Chem. Geol.* **200**, 59–69.

Ono S., Wing B., Johnston D., Farquhar J. and Rumble D. (2006) Mass-dependent fractionation of quadruple stable sulfur isotope system as a new tracer of sulfur biogeochemical cycles. *Geochim. Cosmochim. Acta* **70**, 2238–2252.

Ono S., Shanks, III, W. C., Rouxel O. J. and Rumble D. (2007) ^{33}S constraints on the seawater sulfate contribution in modern seafloor hydrothermal vent sulfides. *Geochim. Cosmochim. Acta* **71**, 1170–1182.

Overmann J. (1997) Mahoney Lake: a case study of the ecological significance of phototrophic sulfur bacteria. *Adv. Microb. Ecol.* **15**, 251–288.

Overmann J., Beatty J. T., Hall K. J., Pfennig N. and Northcote T. G. (1991) Characterization of a dense, purple sulfur bacterial layer in a meromictic salt lake. *Limnol. Oceanogr.* **36**, 846–859.

Overmann J., Beatty J. T., Krouse H. R. and Hall K. J. (1996) The sulfur cycle in the chemocline of a meromictic salt lake. *Limnol. Oceanogr.* **41**, 147–156.

Peduzzi S., Tonolla M. and Hahn D. (2003a) Vertical distribution of sulfate-reducing bacteria in the chemocline of Lake Cadagno, Switzerland, over an annual cycle. *Aquat. Microb. Ecol.* **30**, 295–302.

Peduzzi S., Tonolla M. and Hahn D. (2003b) Isolation and characterization of aggregate-forming sulfate-reducing and purple sulfur bacteria from the chemocline of meromictic Lake Cadagno, Switzerland. *FEMS Microbiol. Ecol.* **45**, 29–37.

Pfennig N. (1975) The phototrophic bacteria and their role in the sulfur cycle. *Plant Soil* **43**, 1–16.

Riccardi A. L. (2007) Carbonate-associated sulfate: assessment of and use as an isotopic proxy for global sulfur cycling during end-permian mass extinction. Ph.D. dissertation, Department of Geosciences, The Pennsylvania State University, State College, Pennsylvania.

Sørensen K. B. and Canfield D. E. (2004) Annual fluctuations in sulfur isotope fractionation in the water column of a euxinic marine basin. *Geochim. Cosmochim. Acta* **68**, 503–515.

Suits N. S. and Wilkin R. T. (1998) Pyrite formation in the water column and sediments of a meromictic lake. *Geology* **26**, 1099–1102.

Sweeney R. E. and Kaplan I. R. (1980) Stable isotope composition of dissolved sulfate and hydrogen sulfide in the Black Sea. *Mar. Chem.* **9**, 145–152.

Takahashi T., Broecker W., Li Y. H. and Thurber D. (1968) Chemical and isotopic balances for a meromictic lake. *Limnol. Oceanogr.* **13**, 272–292.

Thamdrup B., Finster K., Hansen J. W. and Bak F. (1993) Bacterial disproportionation of elemental sulfur coupled to chemical reduction of iron or manganese. *Appl. Environ. Microbiol.* **59**, 101–108.

Thompson J. B. and Ferris F. G. (1990) Cyanobacterial precipitation of gypsum, calcite, and magnesite from natural alkaline lake water. *Geology* **18**, 995–998.

Thompson J. B., Ferris F. G. and Smith D. A. (1990) Geomicrobiology and sedimentology of the mixolimnion and chemocline in Fayetteville Green Lake, New York. *Palaios* **5**, 52–75.

Thompson J. B., SchultzeLam S., Beveridge T. J. and DesMarais D. J. (1997) Whiting events: biogenic origin due to the photosynthetic activity of cyanobacterial picoplankton. *Limnol. Oceanogr.* **42**, 133–141.

Tonolla M., Peduzzi S., Hahn D. and Peduzzi R. (2003) Spatio-temporal distribution of phototrophic sulfur bacteria in the chemocline of meromictic Lake Cadagno (Switzerland). *FEMS Microbiol. Ecol.* **43**, 89–98.

Torgersen T., Hammond D. E., Clarke W. B. and Peng T.-H. (1981) Fayetteville, Green Lake, New York: ^{3}H–^{3}He water mass ages and secondary chemocline structure. *Limnol. Oceanogr.* **26**, 110–122.

Vanuxem L. (1839) Third annual report of the geological survey of the Third District. *Documents of the Assembly of the State of New York, Sixty-Second Session*, vol. 5, pp. 241–285.

Werne J. P., Lyons T. W., Hollander D. J., Formolo M. J. and Damste J. S. S. (2003) Reduced sulfur in euxinic sediments of the Cariaco Basin: sulfur isotope constraints on organic sulfur formation. *Chem. Geol.* **195**, 159–179.

Wilkin R. T. and Barnes H. L. (1997) Pyrite formation in an anoxic estuarine basin. *Am. J. Sci.* **297**, 620–650.

Wortmann U. G., Bernasconi S. M. and Bøttcher M. E. (2001) Hypersulfidic deep biosphere indicates extreme sulfur isotope fractionation during single-step microbial sulfate reduction. *Geology* **29**, 647–650.

Zerkle A. L., Farquhar J., Johnston D. T., Cox R. P. and Canfield D. E. (2009) Fractionation of multiple sulfur isotopes during phototrophic oxidation of sulfide and elemental sulfur by a green sulfur bacterium. *Geochim. Cosmochim. Acta* **73**, 291–306.

Zhang J. Z. and Millero F. J. (1993) The products from the oxidation of H_2S in seawater. *Geochim. Cosmochim. Acta* **57**, 1705–1718.

Zopfi J., Ferdelman T. G., Jorgensen B. B., Teske A. and Thamdrup B. (2001) Influence of water column dynamics on sulfide oxidation and other major biogeochemical processes in the chemocline of Mariager Fjord (Denmark). *Mar. Chem.* **74**, 29–51.

Zopfi J., Ferdelman T. G. and Fossing H. (2004) Distribution and fate of sulfur intermediates – sulfite, tetrathionate, thiosulfate, and elemental sulfur – in marine sediments. In *Sulfur Biogeochemistry – Past and Present* (eds. J. P. Amend, K. J. Edwards and T. W. Lyons). Geological Society of America, Denver.

Associate editor: Timothy W. Lyons